Test-Time Compute for Dense Retrieval: Agentic Program Generation with Frozen Embedding Models

Han Xiao
Jina AI *by* Elastic
han.xiao@jina.ai

arXiv:2605.11374v2 [cs.LG] 13 May 2026

Abstract

Test-time compute is widely believed to benefit only large reasoning models. We show it also helps small embedding models. Since modern embedding models are distilled from LLM backbones, a frozen encoder should benefit from extra inference compute without retraining. Using an agentic program-search loop, we explore 259 candidate inference programs over a frozen embedding API across ninety generations. The entire Pareto frontier collapses onto a single algebra: a softmax-weighted centroid of the local top-K documents interpolated with the query. This default, which introduces no trainable parameters, lifts nDCG@10 statistically significantly across seven embedding-model families spanning a tenfold parameter range, with held-out full-BEIR validation confirming the lift on every model tested.

1 Introduction

Test-time compute has transformed reasoning in generative language models. Best-of-N sampling (Brown et al., 2024), self-consistency (Wang et al., 2023b), and verifier-guided search (Snell et al., 2025; Wu et al., 2025) let a smaller model spend more inference FLOPs to match a larger one along a smooth Pareto curve. The common reading is that this scaling regime is reserved for large reasoning LLMs and that small models have nothing to gain. Dense retrieval, dominated by small embedding models, has not yet been studied through a test-time-compute lens. Frozen embedding models such as `jina-embeddings-v5-text-small` (`j-v5-small`), `e5-base-v2`, and `gte-base-en-v1.5` are deployed with one forward pass per query and one cosine similarity per document.

We argue that the small-model picture is misleading. Most modern embedding models are distilled or initialised from large LLM backbones. `Qwen3-Embedding` (Zhang et al., 2025) starts from the Qwen3 foundation models and inherits their representation space. `EmbeddingGemma` (Vera et al., 2025) is built on Gemma 3 and uses its long-context backbone. `j-v5` (Akram et al., 2026) is distilled from Qwen3 with task-LoRA adapters on top. SFR-Embedding-2 (Meng et al., 2024) is fine-tuned from Mistral-7B. NV-Embed-v2 (Lee et al., 2025) adapts a decoder-only LLM with latent attention. GritLM (Muennighoff et al., 2025) unifies generative and embedding capabilities in a single Mistral-based model. To the extent that test-time compute is a property of the underlying LLM representation space, these distilled small embedding models should inherit at least some of that potential. Existing test-time scaling proposals for retrieval require an external generative LLM (Gao et al., 2023; Wang et al., 2023a), a second supervisory retriever (Uzan et al., 2026), or trained extra parameters (Xiao et al., 2026). This work asks a stricter question: how much can a frozen single-vector embedding model gain at inference, with no auxiliary model and no new parameters?

We answer with an agentic program-search loop in which an LLM agent writes Python programs over the frozen embedding API, a harness scores each candidate on a multi-task retrieval benchmark, and a long-horizon memory accumulates ruled-out hypotheses. Section 3 describes the loop architecture. Section 4 reports the emergent structure of the search output. Section 5 validates the discovered programs on held-out full-BEIR tasks across seven embedding-model families and connects the winning program to classical pseudo-relevance feedback.

2 Related Work

2.1 Test-time compute for generative LLMs

Best-of-N scaling forms the dominant test-time compute paradigm for generative LLMs. Snell et al. (2025) formalize compute-optimal allocation

between best-of-N sampling and iterative revision. Brown et al. (2024) show best-of-N scales coverage log-linearly. Wu et al. (2025) establish a clean inference scaling Pareto frontier on math problem-solving. Wang et al. (2023b) introduce majority-vote over sampled chains-of-thought. Common to all four is stochasticity: sample many noisy candidates, then aggregate. We adopt the same question: whether extra inference compute can substitute for a larger embedding model, and find the embedding analogue is structural rather than stochastic.

2.2 Generation-based query expansion

HyDE (Gao et al., 2023) embeds an LLM-generated hypothetical answer in place of the query; Query2Doc (Wang et al., 2023a) concatenates the LLM expansion to the query before encoding. Both rely on an external LLM at query time, trading inference latency and cost for retrieval gain. Zhuang et al. (2024) prompt LLMs to generate dense+sparse representations directly. We restrict ourselves to the embedding model itself, with no generative model in the inference path.

2.3 Pseudo-relevance feedback

Classical PRF (Rocchio, 1971; Robertson et al., 1995) re-formulates the query using terms from initial top-ranked documents. The de-facto sparse-PRF baseline is RM3 (Lavrenko and Croft, 2001), which interpolates the original query with a relevance language model estimated from pseudo-relevant documents and remains a strong baseline on top of BM25. Learned sparse retrievers such as SPLADE (Formal et al., 2021) likewise rely on lexical expansion.

Recent dense PRF work takes three distinct routes. CEQE (Naseri et al., 2021) operates at the term level via contextualized embeddings. VPRF (Li et al., 2023a) aggregates top-k dense embeddings into a vector-PRF query update. ANCE-PRF (Yu et al., 2021) trains a small reranker to consume top-k embeddings. VPRF is the closest training-free prior art, since it computes a uniform mean over the top-k retrieved-document embeddings and interpolates with the query. Our work can be seen as extending VPRF by replacing the uniform mean with a softmax-temperature-weighted centroid and adding an interpolation coefficient α. VPRF is the $\tau \to \infty$, α=1 limit of SoftCentroid and appears as a data point in our ablation grid. Section 5 validates the full parameterization across 13 tasks and seven embedding-model families.

A separate line of recent vector-PRF extensions brings an LLM into the inference loop, including LLM-VPRF (Li et al., 2025b), GPRF (Tu et al., 2026), and PromptPRF (Li et al., 2025a). These lie in a different inference regime than the training-free, no-LLM substrate explored here. PromptPRF reports that LLM-extracted features over PRF documents narrow the gap between small and large dense retrievers. We observe a similar small-model lift without requiring an LLM in the inference path.

The relationship between the programs discovered by our search and classical PRF is discussed in Section 6.

2.4 Test-time scaling for retrieval

MetaEmbed (Xiao et al., 2026) adds learnable Meta-Tokens that produce a flexible multi-vector representation, scaling accuracy with the number of tokens kept at test time. It requires training. GQR (Uzan et al., 2026) performs gradient descent on the query embedding using a second model's similarity as supervision. It requires a secondary retriever. Both target multimodal hybrid retrieval. Late interaction in ColBERT and ColBERTv2 (Khattab and Zaharia, 2020; Santhanam et al., 2022) is another way to spend more compute per query, but at the cost of multi-vector storage. Our regime is strictly more constrained, requiring a frozen single-vector embedding model, no second model, and no extra forward pass for the cheapest variant.

2.5 Program generation and agentic discovery

Closest to our methodological framing are LLM-driven program-generation loops in which a language model proposes candidate programs, an evaluator scores them, and the surviving programs condition the next round of proposals. FunSearch (Romera-Paredes et al., 2024) discovered new constructions for the cap set problem and bin packing this way. AlphaEvolve (Novikov et al., 2025) extended the pattern to a coding agent capable of improving algorithmic primitives. ELM (Lehman et al., 2024) explored LLM-assisted evolution earlier. Our agent loop is an instance of the same pattern, specialized to embedding-program search. The agent is conditioned on a Pareto frontier over cost and ΔnDCG, plus a structured log of which substrate families the search has already moved beyond. The evaluator is a pinned multi-task retrieval harness. To our knowledge this is the first time this loop has been applied to the dense-retrieval inference recipe.

3 Methodology

The central contribution of this paper is a rerunnable agentic loop that discovers embedding programs for dense retrieval.[1] An LLM agent explores a structured search space of embedding-level operations. A harness scores each candidate on a fixed multi-task retrieval benchmark under a GPU lock. A long-horizon memory accumulates ruled-out hypotheses so the agent does not revisit structurally equivalent ideas. Section 4 reports what the loop produced across ninety generations of search, including the emergent algebraic structure of the Pareto frontier. Section 5 reports the cross-model validation at full-BEIR scale.

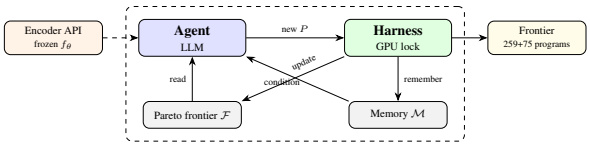

Figure 1: Agentic generation loop. At each round g, the agent reads the Pareto frontier and the long-horizon memory, writes new Python programs over the frozen embedding-model API, and queues them on the harness. The harness evaluates each program under a GPU lock. Surviving programs update the frontier, and all results, both positive and ruled-out, enter the memory. The loop runs unsupervised for ninety rounds.

3.1 Outer loop

The agent runs as a cron-driven generation loop, with one full iteration laid out in Algorithm 1. At the start of each generation g the agent reads three inputs: the current Pareto frontier $\mathcal{F}_{g-1}$ over cost and average ΔnDCG@10; the per-cell evaluation history over six universal cells, defined as two embedding-model sizes by three retained tasks {NFCorpus, SciFact, ArguAna}, with FiQA-2018 evaluated on every program as a separate stress task that does not gate frontier admission; and a structured log of meta-lessons accumulated from prior generations. The agent then writes one or two new programs as Python functions and appends them to a versioned registry `v{g}.py`. A separate runner process acquires a GPU lock, evaluates each newly registered program on all six universal cells over a small hyperparameter sweep, writes results to JSONL, and logs the outcome as HIT, MARGINAL, MISS, or non-universal back into the meta-lesson record for the next generation.

[1] Code, program registry, long-horizon memory, and evaluation harness: https://github.com/hanxiao/embedding-ttc

Algorithm 1 Agentic embedding-program generation loop.

Initialize registry $\mathcal{R} \leftarrow \{P_0\}$ // P_0: cosine baseline
Initialize Pareto frontier $\mathcal{F} \leftarrow \{P_0\}$, long-horizon memory $\mathcal{M} \leftarrow \emptyset$
for generation $g = 1, 2, \ldots, G$ **do**
  $\{P_j^{\text{new}}\}_j \leftarrow \textsc{Propose}(\mathcal{F}, \mathcal{M})$ // LLM writes Python programs
  $\mathcal{R} \leftarrow \mathcal{R} \cup \{P_j^{\text{new}}\}_j$
  for each $P \in \{P_j^{\text{new}}\}_j$, each cell c, each $\theta \in \Theta_P$ **do**
    $\Delta_c \leftarrow \textsc{Evaluate}(P_\theta, c)$ // ΔnDCG@10 vs P_0
  end for
  $\mathcal{F} \leftarrow \textsc{ParetoUpdate}(\mathcal{F}, \mathcal{R})$ // cost vs mean Δ
  $\mathcal{M} \leftarrow \textsc{AppendLessons}(\mathcal{M}, \{\Delta_c\})$ // ruled-out families, meta-lessons
end for
return $\mathcal{F}, \mathcal{R}, \mathcal{M}$

3.2 Proposer

The agent writes Python programs over the frozen embedding model API. It is bound by a four-rule contract. Each new program must touch a substrate family, a named category of embedding-space operations such as centroid replacement, LoRA fusion, or stochastic ensembling, that the long-horizon memory does not mark closed. It must branch on argmax or argpartition or use only structurally fixed thresholds. It must cite at least one of six fixed proposal principles, such as "argmax over confidence, not over output values". And it must justify why the program is not equivalent under composition to any program already in $\mathcal{R}$. The structural-threshold rule prevents the agent from quietly tuning hyperparameters into the program text. The agent is otherwise unconstrained. It may manipulate text, introduce conditional gates, operate in score space, combine LoRA adapters, or compose operations in any order. The agent is free to mutate hyperparameters of an existing program, recombine two parents, or open a new substrate family. Generation-by-generation behaviour is logged in `PROGRAM_LOG.md`.

3.3 Long-horizon memory

The long-horizon memory is the loop's persistent context. Each generation appends which sub-

strate families were ruled out, which compositions are redundant, and which families still have open hypotheses. Two representative entries from `PROGRAM_LOG.md`, surfaced verbatim in the registry conditioning prompt, illustrate the discipline. The first records that stochastic ensembling returns no signal on any of the six universal cells: the median of unit-norm embeddings leaves the unit sphere and there is no verifier to pick a winning sample, unlike LLM best-of-N. The second records that raw-document HyDE with majority gates collapses by construction, because each top-k document viewed as a pseudo-query retrieves itself with similarity one. The memory keeps the agent from revisiting structurally equivalent ideas under new names and is the principal reason the search remains productive across ninety generations.

3.4 Evaluation harness

Programs are evaluated on six universal cells, formed by crossing {`j-v5-small`, `j-v5-nano`} with {NFCorpus, SciFact, ArguAna}, plus FiQA-2018 as an additional stress cell on each embedding model. The four-task baseline reproductions in Appendix Table 10 cover the same eight cells. Each cell runs MTEB v2.8.4 with a fixed dataset revision. These nanoBEIR cells use 50-query sub-samples and serve exclusively for frontier admission during the search. All final claims are validated on full-BEIR corpora with paired bootstrap significance on per-query nDCG@10 using 10,000 resamples. A program is called universal if all six universal cells are non-negative. Otherwise it is recorded but does not enter the frontier.

The cost axis used to admit programs to the frontier is the per-query encoder forward-pass count. Per-query test-time complexity in dense retrieval decomposes into three components. Let F denote the encoder forward-pass cost, N the corpus size, d the embedding dimension, N_c the first-stage candidate pool depth, and K the local centroid radius. The trivial program P_0 runs in $\mathcal{O}(F + dN)$ time for query encoding and dense scoring, or in $\mathcal{O}(F + d \log N)$ when an ANN index replaces the dense scan. A frontier program at $c\times$ encoder cost runs in $\mathcal{O}(cF + dN_c + dK)$. This decomposes into c encoder forward passes for the query and any re-encoded anchors, one $\mathcal{O}(dN_c)$ matrix-vector multiply over the candidate pool to score against the updated query, and an $\mathcal{O}(dK)$ aggregation to compute the centroid. The $\mathcal{O}(cF)$ term dominates because F is roughly 10 to 50 ms per query for transformer encoders, while dN_c is about 0.05 ms at N_c=1000 and d=1024 on a single CPU thread. The cost factor c is therefore the meaningful test-time scaling axis. The agent's frontier is admitted by the pair c and $\Delta\mathrm{nDCG@10}$, with c counted in encoder forward passes.

We track three frontier strata. The $1\times$ stratum requires no extra encoder pass and only matrix-vector arithmetic over precomputed embeddings. The $2\times$ stratum allows one extra encoder pass for an anchor re-encoding. The $\geq 4\times$ stratum allows multiple anchors or LoRA re-encodings. Within $1\times$ all costs are dominated by the $\mathcal{O}(dN_c)$ matrix-vector multiply, which we treat as effectively free. Appendix B reports the empirical scaling of Δ nDCG@10 against c across the registry of 1,522 evaluations. We use "encoder cost" and "encoder forward pass" as standard technical terms throughout, both referring to one forward pass of the embedding model.

Section 4.2 reports the runtime trajectory of the loop, including the cumulative discovery curve and the substrate-family breakdown of programs proposed and ruled out.

4 Discovered Programs

The agent is not constrained to a predefined grammar. Each program is an arbitrary Python function over a minimal interface: a frozen embedding model f_θ mapping text to unit-norm vectors, a precomputed document index D with embeddings $\mathbf{d}_i = f_\theta(d_i)$, and retrieval via $s_i = f_\theta(q)^\top \mathbf{d}_i$. The agent is free to manipulate text through sentence splitting, truncation, and instruction prefixes. It may introduce conditional branching through gap-confidence gates, robustness witnesses, and overlap checks. It may operate in score space using Borda, RRF, or z-score fusion. It may combine multiple LoRA adapters. It may compose these operations in any order. The centroid-algebra finding is non-trivial precisely because the search space is this unconstrained. The rest of this section reports the structure the agent independently re-derived as the simplest hypothesis consistent with the universal-positive criterion across all rounds of search.

4.1 Emergent algebraic structure

Every program on the discovered Pareto frontier is a structured update that moves the query toward a local document centroid, followed by re-ranking with the updated query. Programs in structurally

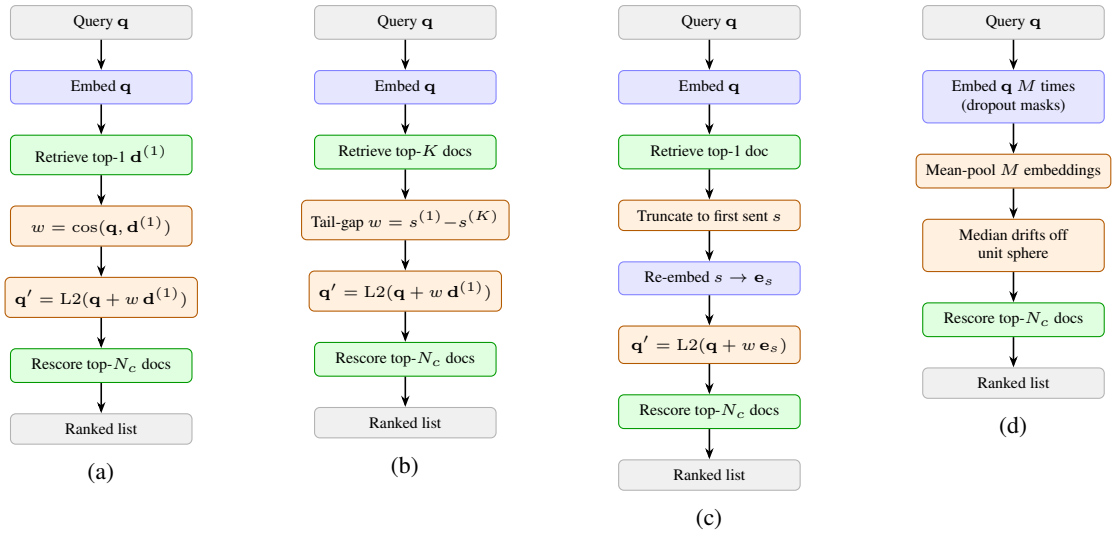

Figure 2: Four representative programs discovered by the agentic loop. (a) P1: top-1 self-amp, founder of the AMP family, cost $1\times$. (b) P32: tail-gap weighted amp, SOFTCENTROID family, cost $1\times$. (c) P19: first-sent anchor, $2\times$-cost frontier holder on ArguAna. (d) P35: dropout ensemble, stochastic sampling baseline, cost $M\times$. Programs (a)–(c) belong to the centroid super-family; (d) mean-pools unit-norm embeddings under dropout.

different families, such as stochastic ensembles, score-space fusion, cascade reranking, asymmetric LoRA encoding, and text perturbation, were explored across ninety rounds of search, and the frontier concentrated exclusively on centroid-algebra programs, sharpening the structural claim by exhausting alternative substrate families.

Post hoc, every frontier program reduces to a composition of five operations:

$$\begin{aligned}
\textsc{enc}(\textit{text};\, \textit{adapter},\, \textit{prefix}) &\to \mathbb{R}^d \\
\textsc{retr}(\mathbf{v};\, D,\, k) &\to \mathcal{T}_k \subseteq \{1, \ldots, N\} \\
\textsc{aggr}(\{\mathbf{d}_i\}_{i \in \mathcal{T}_k};\, \textit{op}) &\to \mathbb{R}^d \\
\textsc{intp}(\mathbf{v}_1,\, \mathbf{v}_2;\, \alpha) &\to \mathbb{R}^d \\
\textsc{rerank}(D';\, \mathbf{q}') &\to \text{ranked list}
\end{aligned}$$

with AGGR parameterized by $\textit{op} \in \{\text{mean}, \text{softmax}_\tau, \text{max}\}$. This is not a search space we defined upfront. It is a finding. The agent explored seventeen substrate families spanning text manipulation, gating, score-space arithmetic, multi-LoRA routing, and stochastic sampling, as Section 4.2 documents. The entire Pareto frontier collapsed into this simple algebra. The baseline is the trivial program $P_0 = \textsc{rerank}(D; \textsc{enc}(q))$. Every frontier program extends it by inserting a retrieve-aggregate-interpolate step between encoding and reranking.

The emergent structure varies along three axes. An aggregation axis selects between mean and softmax-weighted, with or without a similarity floor. An anchor axis selects among top-k document embeddings, a first-sentence pseudo-document, and title-only encoding. A gate axis selects among always-fire, gap-confidence, and robustness-witness conditions. All three axes share the same geometric template: move the query toward a local centroid, then rerank. Representative frontier programs are schematized as flow diagrams in Appendix G.

Three concrete programs ground the empirical sections. The first is embedding-space Rocchio: given the initial query embedding $\mathbf{q} = f_\theta(q)$ and the indices of the top-K retrieved documents $\mathcal{T}_K$, the updated query is

$$\mathbf{q}' = \text{normalize}\left(\mathbf{q} + \beta \cdot \frac{1}{K} \sum_{i \in \mathcal{T}_K} \mathbf{d}_i\right). \qquad (1)$$

We call this ROCCHIO. The only new compute is one $\mathbb{R}^d$ argpartition over N scores, one mean over K vectors, and one extra $\mathbb{R}^d \times \mathbb{R}^{d \times N}$ matrix product. Because $\mathbf{d}_i$ is precomputed, no additional encoder forward pass is needed. We call this $1\times$ encoder cost.

The second program, SOFTCENTROID, replaces the simple mean with a temperature-controlled softmax over initial similarities and interpolates the

query toward the resulting centroid:

$$w_i = \frac{\exp(\mathbf{q}^\top \mathbf{d}_i/\tau)}{\sum_{j\in\mathcal{T}_K} \exp(\mathbf{q}^\top \mathbf{d}_j/\tau)}, \tag{2}$$

$$\mathbf{q}' = \text{normalize}\left((1-\alpha)\mathbf{q} + \alpha \sum_{i\in\mathcal{T}_K} w_i \mathbf{d}_i\right). \tag{3}$$

At α=1 the query is fully replaced by the centroid; at $\tau \to 0$ the centroid collapses to the top-1 document. With α=0.5, τ=0.05, and $K \in \{2, 3\}$, SOFTCENTROID is the strongest $1\times$ program found.

The third program, FIRSTSENT, takes the top-1 retrieved document $d^{(1)}$, truncates it to its first sentence $s^{(1)}$, re-encodes that sentence, and interpolates the query toward the single anchor:

$$\mathbf{q}' = \text{normalize}\Big((1-\alpha)\mathbf{q} + \alpha \cdot f_\theta(s^{(1)})\Big).$$

This costs one additional encoder forward pass per query at $2\times$ encoder cost. The per-corpus first-sentence cache amortizes across queries. The first sentence is extracted from the raw document body via the standard NLTK Punkt sentence tokenizer, not from a preprocessed title or abstract field. On corpora without natural sentence boundaries, such as code and dialogue, this anchor would need to be redefined.

The full set of substrate families the meta-program explored is enumerated in the supplementary alongside the relevant entries from the program log. The list includes LORAFUSION, DOCCHUNK, QUERYTEMPLATE, DROPOUTENS, ASYMLORA, QUERYREPEAT, score-space Borda and RRF, per-LoRA z-score fusion, cascade reranking, and robustness gates.

4.2 Search trajectory

We first examine the program-search trajectory to understand how programs evolve and what compute-accuracy tradeoffs emerge.

The loop ran for ninety generations across roughly three wall-clock days, registering 259 programs across seventeen substrate families and evaluating 10,535 configurations. The agent used Claude Opus 4 with a long-horizon prompt that includes the current Pareto frontier and long-horizon memory. One generation cost approximately 0.30 in API charges and produced one or two new programs. Total agent cost was approximately \$30 over the search. The cumulative discovery curve in Figure 3 flattens after generation 30 and saturates after generation 78, suggesting the $2\times$ universal frontier has been exhausted under the current encoder API. The trajectory reveals three distinct stages.

The search began with the substrates most directly inspired by LLM test-time compute. Cross-task LoRA fusion, dropout-based embedding ensembles, asymmetric LoRA encoding, and multi-prompt query templates are the natural analogues of best-of-N sampling, self-consistency, and prompt engineering. All four were ruled out within the first ten rounds. The long-horizon memory recorded the structural reason in each case. Stochastic ensembling has no verifier to select among samples, so its mean leaves the unit sphere into a metric the model was not trained to respect. Asymmetric LoRA encoding projects queries and documents into misaligned subspaces, which removes the geometric alignment the embedding model relies on. The agent therefore moved on quickly to substrates more aligned with the cosine geometry.

The first successful programs emerged from embedding-space Rocchio, a classical technique the agent independently re-derived. The agent then began systematic variation with similarity floors, multi-round iteration, z-score normalization, and negative feedback. It discovered that replacing the uniform mean with a softmax-temperature-weighted centroid and adding an interpolation coefficient α produced a strictly better default. The SOFTCENTROID family crystallized around generation 25 with K=3, α=0.5, τ=0.05.

In the middle stage, the agent explored alternative anchors including first-sentence re-encoding, title-only encoding, document chunking, corpus-mean subtraction, and pseudo-document replacement. FIRSTSENT became the $2\times$ frontier holder on ArguAna with gains of $+6.9$ to $+7.3$ nDCG@10. Score-space fusion methods and cascade reranking were explored and shown to be dominated by the centroid family. Once the centroid family was established, the agent turned to the question of when to apply programs, through gap-confidence gates, top-K overlap witnesses, and robustness witnesses. These gates modestly improved worst-case behaviour but did not move the universal frontier.

The final twelve rounds covered instruction-prefix queries, document-side projection, title-as-anchor, and composite witnesses. They confirmed

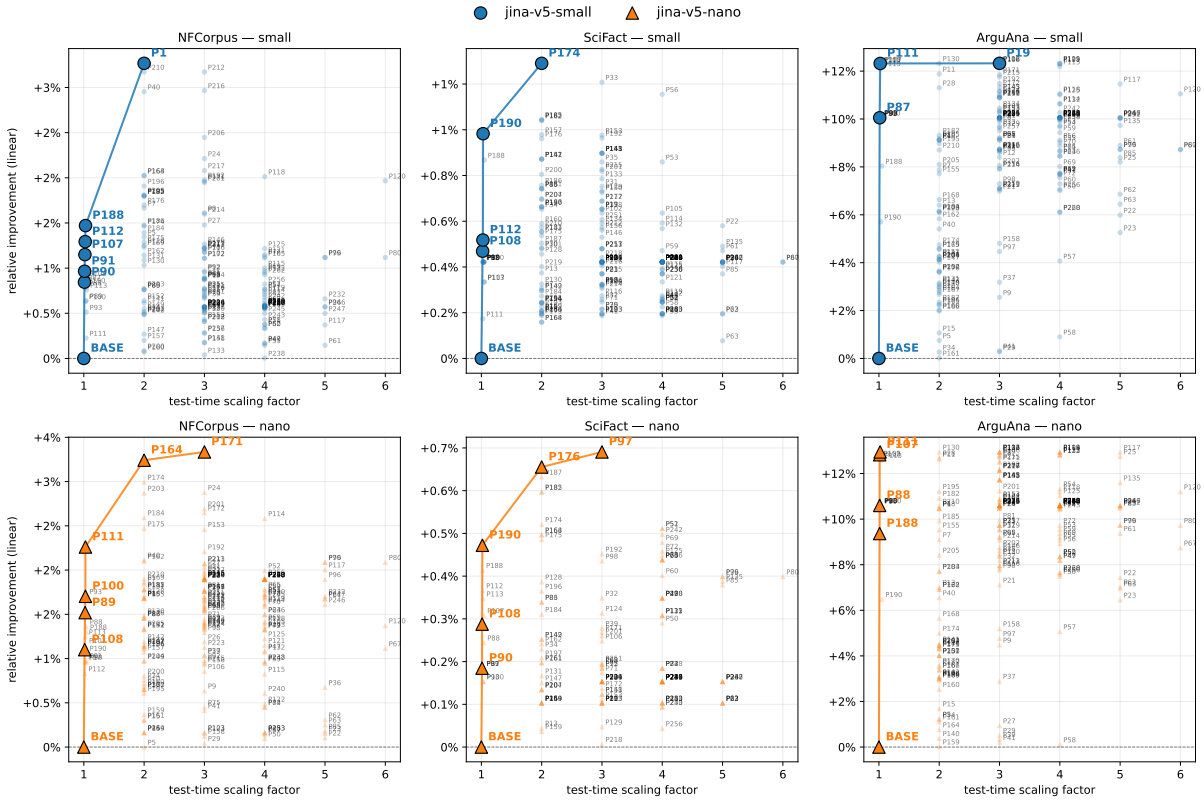

Figure 3: Cumulative best universal ΔnDCG@10 averaged over six cells as a function of generation. Of 259 registered programs, only those with positive mean improvement are plotted; the x-axis truncates at 6× encoder cost because no program beyond that cost improves over the baseline. The curve flattens after generation 30 and saturates after generation 78, suggesting the fixed-program frontier is exhausted. Section 4.4 subsequently opens a new axis by searching over routing policies rather than algebraic primitives.

the saturation of the frontier identified earlier rather than extending it. The long-horizon memory had accumulated 23 meta-lessons by this point, and the agent's novel-substrate rate dropped to zero, signalling a clean stopping point for the search.

The frontier program is one realization of a rerunnable search. Substituting a different embedding-model family, benchmark, or encoder API produces a different frontier under the same loop. The closest existing patterns are FunSearch (Romera-Paredes et al., 2024) and AlphaEvolve (Novikov et al., 2025). The contribution specific to this work is the application surface, training-free dense retrieval, and the long-horizon memory that steers the search toward structurally cleaner programs rather than novelty for its own sake.

4.3 Branching structure

The 259 programs form a directed acyclic graph of parent-child relationships, with each program citing its parents and the mutation or recombination that produced it. The seventeen substrate families cluster into three super-families. The centroid super-family covers ROCCHIO, SOFTCENTROID, FIRSTSENT, ROCCHIO-FLOOR, pseudo-document replacement, and title-anchor variants. It accounts for over 180 frontier-eligible programs whose common structure is a query update toward a local document centroid or anchor, varying in aggregation, anchor source, and gating. The stochastic super-family covers DROPOUTENS, ASYMLORA, QUERYTEMPLATE, QUERYREPEAT, and multi-prompt ensembling. Its 40 or so programs sit uniformly at or below baseline because no verifier exists to select among noisy embedding samples. The score-space super-family covers Borda, RRF, z-score fusion, cascade reranking, and per-LoRA fusion. Its 30 or so programs are occasionally marginal but never universal, because operating in score space rather than embedding space loses the geometric structure that makes centroid updates effective. Representative frontier programs are schematized as flow diagrams in Appendix G.

Of the 259 programs evaluated on the full set of six universal cells, 88 satisfy the strict universal-

positive criterion of $\Delta \geq 0$ on all six cells. A further 55 programs are positive on five of six cells, with mean Δ from $+2.3$ to $+2.7$ nDCG@10. The near-universal cohort overlaps the universal-positive cohort in mean lift, suggesting that strict universality is a conservative admission criterion rather than a tight performance ceiling. The search produces a wide cohort of strong candidates above the trivial program P_0, and the universal default we report is a conservative pick from this cohort.

4.4 Query-adaptive compute routing

SOFTCENTROID applies the same centroid update to every query regardless of its difficulty or type. Since compute-optimal allocation outperforms uniform allocation in LLM reasoning (Snell et al., 2025), we tested whether adaptive routing can further improve the embedding frontier.

The agentic loop then explored 75 additional programs across 26 further generations, seeded with the existing Pareto frontier and long-horizon memory. The agent was instructed to vary the *routing policy* rather than the algebraic primitive. The champion program, ADAPTIVESC, classifies each query into one of three compute tiers based on two signals: query character length and the cosine-score gap between the top-1 and top-K retrieved documents (a confidence proxy).

- **Long queries** (> 350 characters): double SOFTCENTROID pass followed by a first-sentence anchor amplification. Cost $1.5\times$.
- **Medium-length queries with high confidence**: single SOFTCENTROID with a tail-gap boost. Cost $1.0\times$.
- **Short or low-confidence queries**: standard SOFTCENTROID with no additional compute. Cost $1.0\times$.

On the six universal cells (two `j-v5` model sizes by three gated tasks), ADAPTIVESC improves over the fixed SOFTCENTROID default on *every cell*, with a mean lift of $+1.31$ nDCG@10 ($\times 100$) and a minimum of $+0.05$. The largest gains appear on ArguAna ($+3.07$ on `j-v5-small`, $+3.57$ on `j-v5-nano`), where the long symmetric queries trigger the double-SOFTCENTROID path. The aggregate cost is $1.5\times$ the single-forward baseline.

The routing thresholds are model-specific; the centroid algebra itself is unchanged.

Encoder	Task	SC	ADP.SC	ΔSC
`j-v5-small`	NFCorpus	+1.89	+2.43	+0.54
`j-v5-small`	ArguAna	+3.60	+6.67	+3.07
`j-v5-small`	SciFact	+0.13	+0.18	+0.05
`j-v5-nano`	NFCorpus	+1.57	+1.96	+0.39
`j-v5-nano`	ArguAna	+4.02	+7.59	+3.57
`j-v5-nano`	SciFact	+0.24	+0.46	+0.22
Mean		+1.91	+3.22	+1.31
Min		+0.13	+0.18	+0.05

Table 1: ADAPTIVESC versus fixed SOFTCENTROID on `j-v5` universal cells. Values are Δ nDCG@10 ($\times 100$) over the cosine baseline. The ΔSC column shows the per-cell improvement of the adaptive routing over the fixed default. All six cells are positive.

5 Experimental Results

With the search trajectory and emergent algebra established, we now validate whether the discovered programs generalize across tasks, embedding-model families, and corpus scales.

5.1 Experimental setup

The headline embedding models are `j-v5-small` and `j-v5-nano` (Akram et al., 2026), two recent task-LoRA models distilled from Qwen3 that ship four task-specialized adapters over a shared backbone, one each for retrieval, classification, clustering, and text-matching. This adapter design lets us also test cross-task LoRA fusion as a candidate substrate. Models use published HuggingFace weights in fp16. Evaluation uses MTEB v2.8.4 with the official task revisions (Muennighoff et al., 2023; Enevoldsen et al., 2025), and instruction prefixes follow the model card. The four headline retrieval tasks are NFCorpus (Boteva et al., 2016), SciFact (Wadden et al., 2020), ArguAna (Wachsmuth et al., 2018), and FiQA-2018 (Maia et al., 2018), which together span medical IR, scientific fact verification, counter-argument retrieval, and short-question to long-document financial QA, drawn from the BEIR collection (Thakur et al., 2021). Baselines reproduce published nDCG@10 within 0.4 nDCG points on all eight model-by-task cells (Appendix Table 10). Frontier admission during search uses the nanoBEIR dev cells exclusively; held-out validation on full-BEIR corpora and unseen embedding-model families guards against selection bias from the 10,535 evaluated configurations.

All reported numbers use a two-stage pipeline. A first-stage ANN retriever returns a top-N_c candidate pool that the embedding program rescores

against $\mathbf{q}'$. The discovered programs are insensitive to pool depth. Holding the default fixed and varying $N_c \in \{100, \ldots, 5000\}$, SOFTCENTROID reproduces the same Δ nDCG@10 on all representative cells, because the centroid is built only from the local top-K. The rescoring cost is one $d \times N_c$ matrix-vector multiply, around 0.05 ms at N_c=1000 and d=1024 on a single CPU thread, negligible against the 10 to 50 ms encoder forward pass.

Table 2 reports the oracle-best program per cell. To verify this is not overfitting, we run 5-fold random dev/test splits with a 50/50 ratio. The dev-selected SOFTCENTROID configuration retains 80% of oracle gain on `j-v5-small` NFCorpus, 67% on `j-v5-nano` NFCorpus, and 99% and 98% on the two ArguAna cells. On SciFact and FiQA, where oracle gains are below 0.7, dev-selected gains do not survive validation. We therefore restrict claims to NFCorpus and ArguAna.

5.2 Frontier programs on `j-v5`

PRF and centroid replacement dominate on NFCorpus, SciFact, and ArguAna across both models. Table 2 reports the best per-cell program. Symmetric retrieval admits the largest gains. On ArguAna, the smaller `j-v5-nano` embedding model running a length-3 FIRSTSENT program outperforms the 2.8×-larger `j-v5-small` embedding model's single-forward baseline. The same program also lifts `j-v5-small`. The effect is program-level test-time compute substituting for embedding-model size on tasks whose query and document distributions coincide.

The recommended default fixes K=3 as the grid median, α=0.5 as the Rocchio midpoint, and τ=0.05 as the lowest stable temperature. Paired-bootstrap resampling on per-query nDCG@10 with 10,000 resamples avoids post-hoc selection bias. The default lifts NFCorpus by +2.37 on `j-v5-small` and +1.99 on `j-v5-nano`, ArguAna by +2.80 and +3.19, all at $p < 0.001$. SciFact and FiQA gains are within noise. The default never hurts by more than 0.6 nDCG@10 on any of the four tasks.

Table 3 applies the frozen default across all 13 nanoBEIR retrieval tasks (Zeta Alpha, 2024). Nine of the thirteen tasks are strictly held out from the search. The median lift is +0.17 on `j-v5-small` and +0.27 on `j-v5-nano`. HotpotQA on `j-v5-small` is the only cell significant in the negative direction at $p < 0.05$; the same ArguAna cell that shows −2.16 here yields +3.19 at $p < 0.001$ on the full corpus in Table 2, consistent with 50-query sub-sample noise.

The HotpotQA and NQ regressions in Table 3 reveal a structural limitation: SOFTCENTROID does not distinguish factoid questions ("How many goals did X score?") from argumentative or descriptive queries where centroid feedback is beneficial. A further round of the agentic search targets this gap by exploring routing programs on all 13 nanoBEIR tasks. The agent identifies a strong-factoid detector based on a fixed regular expression:

> *factoid* ← query starts with {when (was/is/...), who (was/founded/...), where (was/is/...), which (country/year/...), what (year/city/name/...), how (many/much/long/old/...)}

Factoid queries are routed to plain cosine; all others to SOFTCENTROID (K=3, α=0.524, τ=0.05). No encoder calls are added; the program operates entirely in embedding space (1.0× cost). We call this program FACTOIDROUTE.

Table 4 reports results on all 26 cells (13 tasks × 2 model variants). FACTOIDROUTE is positive versus SOFTCENTROID on 20 of 26 cells, with a mean ΔSC of +0.25 and minimum of −0.29. The QA regressions present in plain SOFTCENTROID are substantially recovered: HotpotQA improves by +0.98 (`j-v5-small`) and +0.35 (`j-v5-nano`); NQ improves by +1.21 and +0.62. Tasks where SOFTCENTROID was already positive remain non-negative in all but two cells (DBPedia −0.19, −0.29), and no cell regresses by more than 0.3 nDCG@10.

FiQA-2018 is the short-finance-question to long-financial-document cell, where the global K=3 default lands closest to baseline on the nanoBEIR slice. A targeted re-sweep along K alone produced larger gains on the 50-query nano slice but those slice-sized gains do not replicate at full-BEIR scale on the same embedding models. Paired-bootstrap stat-sig on per-query nDCG@10 reveals that the K=10 SOFTCENTROID variant is statistically significantly negative on full-BEIR FiQA for both `j-v5-small` at p=.022 and `j-v5-nano` at p=.0002, reinforcing the model-specificity finding that K=10 belongs to monolithic embedding models rather than the multi-LoRA `j-v5` family.

Two negative entries from the same nano sweep sharpen the picture. A five-prefix max-pool ensemble lands below baseline on both models, since the retrieval-LoRA already absorbs query-intent prefixing. A 1.5×-cost last-paragraph PRF program is

Model	Task	Baseline	+ Program	Δ	Cost	Best frontier program
j-v5-nano	NFCorpus	38.75	**40.84**	+2.08	1×	SOFTCENTROID K=2, α=0.5, τ=0.05
j-v5-nano	SciFact	75.91	76.38	+0.47	1×	ROCCHIO-FLOOR K=2, β=0.5, τ=0.75
j-v5-nano	ArguAna	65.63	**72.97**	+7.34	2×	FIRSTSENT K=1, α=0.5
j-v5-nano	FiQA-2018[§]	58.19	60.07	+1.88[§]	1×	SOFTCENTROID K=10
j-v5-small	NFCorpus	39.76	**42.19**	+2.43	1×	SOFTCENTROID K=3, α=0.5, τ=0.05
j-v5-small	SciFact	76.59	77.80	+1.21	4×	DOCCHUNK first-last-mid, max
j-v5-small	ArguAna	64.71	**71.64**	+6.93	2×	FIRSTSENT K=1, α=0.45
j-v5-small	FiQA-2018[§]	63.63	64.63	+0.99[§]	1×	SOFTCENTROID K=5, α=0.35
Cross-model full-BEIR validation, default SOFTCENTROID (K=3, α=0.5, τ=0.05):						
e5-base-v2	NFCorpus	35.47	36.85	+1.30[‡]	1×	(default)
e5-base-v2	SciFact	72.04	72.41	+0.37	1×	(default)
e5-base-v2	**ArguAna**	44.62	**54.95**	**+10.38**[‡]	1×	(default)
e5-base-v2	FiQA-2018	39.85	40.32	+0.47	1×	(default)
Default SOFTCENTROID (K=3, α=0.5, τ=0.05), no per-task tuning:						
j-v5-nano	NFCorpus	38.75	40.81	+1.99[‡]	1×	(default)
j-v5-nano	ArguAna	65.63	68.82	+3.19[‡]	1×	(default)
j-v5-small	NFCorpus	39.76	42.14	+2.37[‡]	1×	(default)
j-v5-small	ArguAna	64.71	67.51	+2.80[‡]	1×	(default)

Table 2: Headline frontier results, reporting nDCG@10 ×100. Top block: oracle-best per-cell frontier program discovered by the meta-program from 10,535 evaluated configurations on the four-task nanoBEIR slices used to gate the loop's frontier admission. Middle block: default SOFTCENTROID at K=3, α=0.5, τ=0.05 applied with no per-task tuning, on full BEIR for the j-v5 family. Bottom block: cross-model full-BEIR validation on e5-base-v2. Significance: [‡] $p < 0.001$, [†] $p < 0.01$ on a paired bootstrap with 10,000 resamples on per-query nDCG@10. "Cost" counts encoder forward passes. [§] Nano-slice FiQA gains do not survive at full-BEIR scale on the j-v5 family. The full-corpus FiQA evidence is on e5-base-v2 in the bottom block at +0.47.

asymmetric across model sizes, lifting j-v5-nano but hurting j-v5-small.

5.3 Parameter sensitivity and compute regimes

A one-parameter ablation around the SOFTCENTROID default reveals that interpolation α and softmax temperature τ carry most of the gain. Low τ adds +2.5 to +2.9 on ArguAna, and moving from α=0.2 to α=0.5 adds +0.6 to +1.8. Centroid size K is largely inert, with ≤ 0.5 across $K \in \{3, 5, 8\}$. Appendix D reports the full grid. Two compute regimes account for all meaningful gains. In the 1× regime, extscSoftCentroid uses no extra encoder forward pass: all operations are matrix-vector arithmetic over precomputed embeddings, adding sub-millisecond overhead per query. This regime delivers all NFCorpus and SciFact gains and most of ArguAna. In the 2× regime, extscFirstSent re-encodes the first sentence of the top-retrieved document, incurring one additional encoder forward pass per query. This regime buys an additional +0.6 to +0.8 nDCG@10 on ArguAna only. Beyond 2×, the frontier gain is marginal. Table 11 show that the cost-accuracy curve is concave and flattens hard above 2×, in contrast to the log-linear best-of-N scaling reported for generative LLMs (Brown et al., 2024). The best mean Δ nDCG@10 is +2.65 at 2×, +2.67 at 3 to 4×, and +2.51 at 5 to 9× across the agent's full registry of 1,522 program-task evaluations.

5.4 Cross-model transfer

We next test whether programs discovered on one embedding-model family transfer to architecturally distinct models at different parameter scales.

The default SOFTCENTROID transfers to five monolithic embedding-model families at full-BEIR scale: the e5 family at three sizes e5-small-v2, e5-base-v2, and e5-large-v2 (Wang et al., 2022); gte-base-en-v1.5 (Li et al., 2023b); and bge-large-en-v1.5, evaluated on the four retrieval headlines plus NQ where data permits. The default lifts ArguAna by ten nDCG@10 points on e5-base-v2 and by three points on gte-base-en-v1.5, both at $p < 0.0001$. NF-

	j-v5-small			j-v5-nano		
Task	Base	Δ	p	Base	Δ	p
NFCorpus	37.76	$+\mathbf{3.20}^{*}$	.014	35.96	+1.18	.31
SCIDOCS	45.99	$+\mathbf{1.58}$	.13	44.60	+0.32	.73
ArguAna	60.65	+0.28	.69	62.97	−2.16	.07
Touche2020	59.49	+0.58	.36	62.04	+1.02	.24
FiQA-2018	63.63	+0.51	.41	58.19	+0.30	.81
DBPedia	67.49	+0.38	.67	67.02	+0.34	.65
Quora	96.33	+0.17	.42	97.09	+0.27	.15
MSMARCO	65.04	+0.16	.83	65.73	−0.07	.94
FEVER	94.46	−0.05	.77	93.26	−0.14	.53
ClimateFEVER	43.42	−0.17	.85	42.27	+0.52	.65
SciFact	80.90	−0.95	.45	82.33	−2.12	.12
NQ	73.78	−2.28	.16	75.79	−2.17	.07
HotpotQA	84.67	-3.24^{*}	.014	81.28	−1.21	.12
Mean	67.20	+0.01	—	66.81	−0.30	—
Median	65.04	+0.17	—	65.73	+0.27	—
Sig. ($p < .05$)	+1 / −1			0 / 0		

Table 3: Small-sample generalization probe with the default SOFTCENTROID at K=3, α=0.5, τ=0.05 frozen across all 13 nanoBEIR retrieval tasks on both models. NanoBEIR is a 50-query random sub-sample of each BEIR task. Paired-bootstrap p-values use 10,000 resamples on per-query nDCG@10. At this sample size, per-cell p-values are noisy. Deltas that conflict in sign with the full-corpus evaluation, for example ArguAna on `j-v5-nano` at −2.16 here against +3.19 on the full 1,406-query corpus in Table 2, are non-significant at p=.07. Bold marks the single cell significant at $p < .05$. HotpotQA on `j-v5-small` at −3.24, p=.014 is the only statistically significant regression across both models. On `j-v5-nano` no cell crosses the 95% bar.

	j-v5-small			j-v5-nano		
Task	SC	FR	Δ	SC	FR	Δ
NFCorpus	41.22	41.37	+0.15	37.17	37.20	+0.04
SCIDOCS	47.49	47.97	+0.48	44.74	44.76	+0.02
Touche2020	59.90	60.15	+0.25	62.83	62.96	+0.13
ArguAna	69.56	69.59	+0.04	70.66	71.17	+0.51
MSMARCO	65.18	65.40	+0.22	65.67	66.32	+0.65
ClimateFEVER	43.44	43.48	+0.05	42.47	42.70	+0.23
Quora	96.49	96.60	+0.11	97.36	97.31	−0.05
FiQA-2018	63.69	63.69	+0.00	58.49	59.15	+0.67
FEVER	94.40	94.40	+0.00	93.12	93.47	+0.36
SciFact	79.95	79.87	−0.08	80.21	80.25	+0.04
DBPedia	68.25	68.07	−0.19	67.27	66.97	−0.29
NQ	71.50	72.70	+1.21	74.29	74.90	+0.62
HotpotQA	81.28	82.26	+0.98	80.08	80.43	+0.35
Mean			+0.25			+0.25

Table 4: FACTOIDROUTE (FR) vs. SOFTCENTROID (SC) on all 13 nanoBEIR tasks. nDCG@10 (×100). FR routes strong-factoid queries to plain cosine and all others to SOFTCENTROID (K=3, α=0.524, τ=0.05). Rows below the mid-rule are the QA tasks where SC regresses most: FR recovers the majority of the loss. 20/26 cells positive vs. SC. Cost: 1.0× (no extra encoder calls).

Corpus lifts by over one point on both models at $p < 0.001$. Both models reach two of four cells at $p < 0.05$ on full BEIR. SciFact and FiQA-2018 are weaker, as Table 5 records. Combined with the `j-v5` full-BEIR rows in Table 2, NFCorpus and ArguAna lift positively under default SOFTCENTROID on all seven embedding-model families tested at full-BEIR scale.

The optimal cluster size K varies along a clean structural line. The multi-LoRA `j-v5` family prefers K=3 on the 13-task nanoBEIR suite, while both monolithic embedding models we test prefer K=10. At the 13-task scale, the K=10 variant produces positive deltas on 10 of 13 nanoBEIR retrieval cells on `e5-base-v2`, with the largest gains on MS MARCO and ClimateFEVER, as recorded in Appendix F. One reading is that the retrieval LoRA on `j-v5` produces sharper local clusters where K=3 already covers the relevant centroid mass, while monolithic BERT-base embedding models with instruction prefixes produce more diffuse clusters that benefit from a wider K. The algebra and the qualitative finding transfer across all seven embedding-model families.

A parameter-scale ladder on the e5 family at full-BEIR shows the algebra is robust across model sizes within a family, as Table 5 reports. The headline ArguAna lift is approximately stable at eight to ten nDCG@10 points across a tenfold parameter range from `e5-small-v2` at 33M to `e5-large-v2` at 335M. `bge-large-en-v1.5` confirms the algebra also works on a larger member of the BGE family. The earlier weakness on `bge-base-en-v1.5` is therefore a model-specific gap rather than a parameter-scale lower bound. `e5-small-v2` at the same 33M parameter count as `bge-small-en-v1.5` is fully positive on three of four cells, while `bge-small-en-v1.5` is the boundary case where only K=10 on FiQA and ArguAna lifts the baseline. The 4-task nanoBEIR cross-model probe across the three BGE-family models appears in Appendix F.2, Table 18.

The lift also survives on held-out tasks at full-BEIR scale. On SCIDOCS with `e5-base-v2`, SOFTCENTROID gains +0.54 at p=0.016 and fusion raises the total to +1.17 at p=0.0001. The pattern transfers across `e5-large-v2`, `gte-base-en-v1.5`, and `bge-large-en-v1.5`, all at p<0.001. On Touche2020, a BM25-favorable task, pure SOFTCENTROID is non-significant

Encoder	Cell (n_q)	base	SC	SC_{K10}	$\text{SC}_{K5,\alpha.35}$
`e5-base-v2`	NFCorpus (323)	35.47	$+\mathbf{1.30}^{\ddagger}$	$+0.30$	$+\mathbf{0.97}^{\dagger}$
	SciFact (300)	72.04	$+0.37$	-0.36	-0.21
	ArguAna (1406)	44.62	$+\mathbf{10.38}^{\ddagger}$	$+\mathbf{7.08}^{\ddagger}$	$+\mathbf{7.75}^{\ddagger}$
	FiQA-2018 (648)	39.85	$+\mathbf{0.47}$	-0.41	$+\mathbf{0.40}$
	NQ (3452)	58.19	$+\mathbf{0.21}$	-0.58	$+\mathbf{0.24}$
	SCIDOCS (1000)	18.63	$+\mathbf{0.52}$	$+\mathbf{0.27}$	$+\mathbf{0.45}$
	Mean / pos cells	—	$+\mathbf{2.21}/6/6$	$+1.05/3/6$	$+\mathbf{1.60}/5/6$
`gte-base-en-v1.5`	NFCorpus (323)	37.91	$+\mathbf{1.52}^{\ddagger}$	$+\mathbf{0.57}^{*}$	$+\mathbf{0.83}^{\dagger}$
	SciFact (300)	76.19	-0.35	-0.78	-0.80
	ArguAna (1406)	57.24	$+\mathbf{2.87}^{\ddagger}$	$+\mathbf{1.32}^{\ddagger}$	$+\mathbf{1.77}^{\ddagger}$
	FiQA-2018 (648)	40.71	-0.42	$-1.36^{\ddagger}$	-0.39
	Mean / pos cells	—	$+\mathbf{0.91}/2/4$	$-0.06/2/4$	$+0.35/2/4$
`e5-small-v2`	NFCorpus (323)	32.45	$+\mathbf{0.59}$	$+\mathbf{0.37}$	$+\mathbf{0.52}$
	SciFact (300)	68.54	$+\mathbf{0.52}$	-0.61	$+\mathbf{0.25}$
	ArguAna (1406)	41.94	$+\mathbf{8.13}$	$+\mathbf{4.56}$	$+\mathbf{5.92}$
	FiQA-2018 (648)	37.50	-0.04	-0.66	-0.38
	Mean / pos cells	—	$+\mathbf{2.30}/3/4$	$+0.91/2/4$	$+1.58/3/4$
`e5-large-v2`	NFCorpus (323)	37.29	$+\mathbf{1.63}$	$+\mathbf{0.81}$	$+\mathbf{1.26}$
	SciFact (300)	72.17	-0.61	$+\mathbf{0.31}$	$+\mathbf{0.33}$
	ArguAna (1406)	46.38	$+\mathbf{8.81}$	$+\mathbf{6.19}$	$+\mathbf{7.18}$
	FiQA-2018 (648)	41.19	-0.60	-0.91	-0.58
	Mean / pos cells	—	$+\mathbf{2.31}/2/4$	$+1.60/3/4$	$+2.05/3/4$
`bge-large-en-v1.5`	NFCorpus (323)	38.07	$+\mathbf{1.31}$	$+\mathbf{0.57}$	$+\mathbf{0.98}$
	SciFact (300)	74.57	$+\mathbf{0.22}$	-0.31	-0.19
	ArguAna (1406)	64.46	$+\mathbf{3.87}$	$+\mathbf{3.69}$	$+\mathbf{3.32}$
	FiQA-2018 (648)	44.94	-0.10	-0.44	-0.12
	Mean / pos cells	—	$+\mathbf{1.33}/3/4$	$+0.88/2/4$	$+1.00/2/4$

Table 5: Cross-model validation at full-BEIR scale on five monolithic embedding-model families across a tenfold parameter range. The table reports Δ nDCG@10 ($\times 100$) of SoftCentroid default K=3, α=0.5, τ=0.05 and two FiQA-tuned variants. Significance: * $p < 0.05$, † $p < 0.01$, ‡ $p < 0.001$ on a paired bootstrap with 10,000 resamples on per-query nDCG@10, reported on the four cells with stat-sig analysis. NFCorpus and ArguAna lift positively and statistically significantly on the e5 and gte families with the default at $\geq$ 100M. The algebra also extends to `e5-small-v2` at 33M with no model-quality penalty, with ArguAna at $+8.13$, around seven times larger than the corresponding `bge-small-en-v1.5` gain at the same 33M. Combined with the `j-v5` results in Table 2, default SoftCentroid produces positive Δ on NFCorpus and ArguAna across all seven embedding-model families tested at full-BEIR scale, namely `j-v5-small`, `j-v5-nano`, `e5-small-v2`, `e5-base-v2`, `e5-large-v2`, `gte-base-en-v1.5`, and `bge-large-en-v1.5`. `bge-base-en-v1.5` is the only $\geq$ 100M case where the algebra is partial.

but fusion at w=0.1 lifts $+4.93$ to $+5.28$ across embedding-model families, all at p<0.01. The full eight-cell held-out matrix is consolidated in Appendix Table 13.

5.5 Comparison with classical Rocchio and PRF baselines

To isolate the contribution of the softmax-weighted centroid over the classical uniform-mean baseline, we compare SoftCentroid against Rocchio at parity.

Classical Rocchio (Rocchio, 1971) is the strongest training-free dense PRF baseline and is mathematically equivalent to the uniform-mean vector PRF of Li et al. (2023a). To position SoftCentroid against this baseline at parity, we grid sixteen classical-Rocchio configurations over $K \in \{2, 3, 5, 10\}$ and $\beta \in \{0.1, 0.3, 0.5, 0.7\}$ across all 13 nanoBEIR tasks on both models, then compare SoftCentroid against the best Rocchio per cell.

Table 6 and Figure 4 report the comparison on full-BEIR ArguAna across all seven embedding-model families. The softmax-weighted SoftCentroid default exceeds the best Rocchio configuration on every model by $+2.31$ to $+6.00$ nDCG@10, every cell at $p < 10^{-4}$. On NFCorpus, SciFact, and FiQA-2018 the two methods land within one nDCG@10 point. The separation concentrates on symmetric retrieval, where the cosine geometry favours centroid replacement.

Beyond classical Rocchio and sparse PRF, Ap-

Encoder	best Rocchio	SC	SC advantage
e5-small-v2	+5.68	+9.47	+3.79
e5-base-v2	+6.55	+12.55	+6.00
e5-large-v2	+4.99	+10.27	+5.28
gte-base-en-v1.5	+1.25	+3.56	+2.31
bge-large-en-v1.5	+1.13	+5.03	+3.90
j-v5-small	+0.93	+4.74	+3.81
j-v5-nano	+1.22	+5.64	+4.42

Table 6: SOFTCENTROID versus best classical Rocchio on full-BEIR ArguAna across all seven embedding-model families. Each value is Δ nDCG@10 ($\times 100$) over the cosine baseline. The Rocchio number is the best of a sixteen-cell (K, β) grid. SC uses the universal default $K{=}3, \alpha{=}0.5, \tau{=}0.05$. All 14 method-model cells are statistically significant at $p < 10^{-4}$ on a paired bootstrap with 10,000 resamples. The softmax-weighted variant exceeds the uniform-mean baseline on every model by +2.31 to +6.00 nDCG@10.

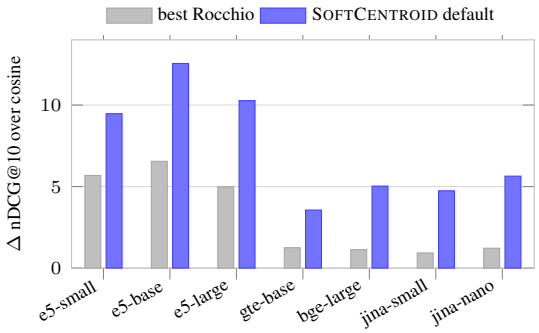

Figure 4: ArguAna full-BEIR lift on each of the seven embedding-model families. SOFTCENTROID at the universal default $K{=}3, \alpha{=}0.5, \tau{=}0.05$ exceeds the best classical Rocchio configuration on every model. Every bar is statistically significant at $p < 10^{-4}$ on a paired bootstrap with 10,000 resamples.

pendix E compares SOFTCENTROID against four additional training-free baseline families: alternative centroid-weighting schemes (uniform, linear, cosine$^{\gamma}$, hard top-1), Rocchio with explicit negative centroids, iterative multi-pass query refinement, and dimension masking. Across 288 cells spanning three encoder families and four BEIR tasks, no alternative consistently outperforms SOFTCENTROID. The softmax temperature is the decisive design parameter: uniform and linear weighting trail by 1.0–1.1 nDCG@10 on average, and Rocchio with negative-centroid subtraction trails by 1.1 nDCG@10. Iterative refinement with fresh re-retrieval at each round yields marginal gains on ArguAna (+2.3 nDCG@10 over SOFTCENTROID at 2× cost) but regresses on SciFact and FiQA. Dimension masking in the style of ECLIPSE/DIME damages retrieval across all cells, with contrastive subtraction losing 5–7 nDCG@10.

5.6 Sparse-dense score fusion

Sparse pseudo-relevance feedback offers a parallel comparison. We implement RM3 (Lavrenko and Croft, 2001) on full-BEIR NFCorpus and SciFact. BM25+RM3 still trails the dense baseline by 8.00 nDCG@10 on NFCorpus and 16.60 on SciFact, both at $p < 10^{-4}$. Dense+SOFTCENTROID leads BM25+RM3 by over 9 nDCG@10 on both tasks. Sparse PRF inherits the BM25 ceiling; the centroid update operates in the embedding space the model was trained for, while RM3 operates over surface terms. The strongest learned-sparse baseline SPLADE+RM3 also trails dense+SOFTCENTROID on both tasks.

The centroid algebra addresses the dense-retrieval side of the inference recipe. A complementary lexical signal can extend the gains to tasks where pure dense retrieval underperforms.

The geometric ceiling identified in Section 6 bounds what centroid replacement alone can achieve under a frozen single-vector embedding model. A natural orthogonal lever injects a lexical signal alongside the dense ranking. BM25 (Robertson et al., 1995) captures rare-term and exact-match cues that cosine similarity in a learned embedding space can underweight. We adopt score-level fusion rather than the alternative two-stage baseline in which BM25 provides the candidate pool and the dense scorer reranks within it.

The two-stage alternative loses substantial accuracy. On full-BEIR e5-base-v2 NFCorpus, the BM25-top-100-then-dense-rerank pipeline regresses by −4.18 nDCG@10 versus the dense baseline at $p < 10^{-4}$, because a BM25 first stage excludes dense-recoverable relevant documents.

We therefore evaluate SOFTCENTROID stacked with min-max-normalized BM25 score fusion on all four full-BEIR headline tasks with e5-base-v2, as Table 7 reports. The fused score is $(1{-}w) \cdot \widetilde{s}_{\text{dense}} + w \cdot \widetilde{s}_{\text{BM25}}$ for a small fusion weight $w{=}0.1$, applied both to the top-K selection feeding the centroid and to the final ranking.

Fusion lifts the mean across the four headline cells from +2.52 to +3.70 nDCG@10. The increment over pure SOFTCENTROID is statistically significant on three of four cells. SciFact and FiQA-2018 move from statistical noise under pure SC into the $p{<}0.01$ regime once fusion is added, while ArguAna is already saturated by the centroid up-

Cell (n_q)	SC pure	SC+fusion	Net (vs. SC)
NFCorpus (323)	+1.11	**+1.95**‡	+0.85*
ArguAna (1,406)	+8.70	**+8.73**	+0.03
SciFact (300)	+0.25	**+2.44**†	+2.19†
FiQA-2018 (648)	+0.01	**+1.69**†	+1.67‡
Mean	+2.52	**+3.70**	+1.18

Table 7: Score-fusion lever on `e5-base-v2` full-BEIR. The table reports Δ nDCG@10 ($\times$100) of pure SOFTCENTROID at K=3, α=0.5, τ=0.05 versus SOFTCENTROID composed with min-max-normalized BM25 score fusion at w=0.1. Significance: * $p < 0.05$, † $p < 0.01$, ‡ $p < 0.001$ on a paired bootstrap with 10,000 resamples on per-query nDCG@10. The "Net gain" column tests the increment of fusion over pure SOFTCENTROID for the same baseline. Fusion lifts every cell. SciFact and FiQA-2018 move from flat under pure SOFTCENTROID into highly significant territory, and the increment over pure SC is statistically significant on three of four cells.

date alone.

The construction transfers across embedding-model families and across a tenfold parameter-scale ladder within the e5 family. Table 8 reports the fusion increment over pure SOFTCENTROID on five monolithic embedding models. The increment is statistically significant on every cell of the e5 parameter ladder at 33M, 110M, and 335M, with nine of nine cells at p<0.05, and on at least one cell per model across all five.

Encoder (params)	NFCorpus	SciFact	FiQA-2018
`e5-small-v2` (33M)	+1.98‡	+3.72‡	+2.88‡
`e5-base-v2` (110M)	+0.85*	+2.19†	+1.67‡
`e5-large-v2` (335M)	+0.82*	+2.46†	+3.56‡
`gte-base-en-v1.5` (110M)	+0.63	+0.50	+1.57‡
`bge-large-en-v1.5` (335M)	+0.14	+1.83†	+1.12*

Table 8: Cross-model fusion increment in Δ nDCG@10 ($\times$100), comparing SC+BM25 fusion at w=0.1 against pure SOFTCENTROID on full-BEIR cells. Significance: * p<0.05, † p<0.01, ‡ p<0.001 on a paired bootstrap with 10,000 resamples. The increment is significant on every cell of the e5 parameter ladder and on at least one cell for every model tested.

The fusion lever generalizes broadly. On `e5-base-v2` 13-task nanoBEIR, the same w=0.1 fusion produces a positive Δ on 12 of 12 retrieval tasks at p<0.0001 pooled. QA-leaning cells that are non-positive under pure SC, including HotpotQA and NQ, all flip positive under fusion. The same pattern holds on `bge-large-en-v1.5` with 11 of 12 tasks positive, confirming that the breadth of the lift is a property of the fusion construction rather than of `e5-base-v2` specifically.

Per-query analysis confirms the lift is broad-based. On NFCorpus, the count of queries improved by SC+fusion exceeds the count regressed on every model tested. The lift is also a retrieval-breadth effect: on `e5-base-v2` NFCorpus, Recall@100 rises from 0.318 to 0.359 under fusion ($p < 10^{-4}$), and the Recall@100 increment exceeds the nDCG@10 increment across all four embedding-model families tested, indicating that new relevant documents enter the top hundred rather than existing ones being reordered within the top ten.

The weight w=0.1 sits inside a wide stable region. On full-BEIR `e5-base-v2` NFCorpus the lift is significant at $p < 0.01$ for all $w \in [0.05, 0.20]$, and the same pattern reproduces on `e5-large-v2`, `bge-large-en-v1.5`, and `gte-base-en-v1.5`. The two parameters K and w are geometrically orthogonal: K controls centroid breadth while w controls lexical injection, and varying K within $\{2, 3\}$ at fixed w=0.10 changes the lift by at most 0.3 nDCG@10.

5.7 Frontier by substrate family

Table 9 groups all programs by substrate family on `j-v5-small`. The centroid families dominate: ROCCHIO, SOFTCENTROID, and FIRSTSENT are the consistent winners. Three non-centroid families, LORAFUSION, DROPOUTENS, and ASYMLORA, do not contribute to the frontier.

5.8 Regimes of test-time compute

The experimental evidence across seven embedding-model families, thirteen retrieval tasks, and two held-out benchmarks converges on a unified geometric picture.

The cosine paradigm is not erased by test-time compute, only wrapped. Three regimes emerge from the discovered frontier: the paradigm breaks on symmetric retrieval, bends on medical-IR headlines, and holds on QA-leaning asymmetric tasks. Figure 5 summarizes this taxonomy across the four headline tasks and the two embedding-model families.

The paradigm breaks on symmetric retrieval. On ArguAna, frontier programs gain six to seven nDCG@10 points over the cosine baseline on `j-v5-small` and `j-v5-nano`, with 99% retention under dev/test validation. On a second embedding-model family, the same default SOFTCENTROID

Family (best variant)	NFC	Sci	Arg	FiQA
1× encoder cost				
ROCCHIO	+1.03	+0.49	+0.60	−0.31
ROCCHIO-FLOOR	+2.18	+0.69	+3.48	−0.12
ROCCHIO K=1	−0.12	−3.16	+6.37	−4.31
SOFTCENTROID	**+2.43**	+0.59	+6.19	−0.30
2× encoder cost				
FIRSTSENT	+1.43	+0.53	**+6.90**	−1.45
QUERYEXPAND	+1.97	+0.36	+3.44	+0.05
LORAFUSION	−0.02	−0.32	+0.15	+0.00
QUERYREPEAT	+0.00	+0.20	+0.22	+0.55
ANSWERTMPL	+0.56	+0.48	+0.32	+0.20
≥ 4× encoder cost				
DOCCHUNK	+0.29	**+1.21**	—§	—§
Anti-patterns (best of family)				
DROPOUTENS	+0.05	+0.28	+0.04	+0.00
ASYMLORA	−3.40	−6.90	−4.06	−7.25

Table 9: Best per-(family, task) Δ nDCG@10 (×100) on `j-v5-small`. Bold marks the all-family winner per column. § marks not applicable, since DOCCHUNK requires long structured documents and ArguAna and FiQA lack this.

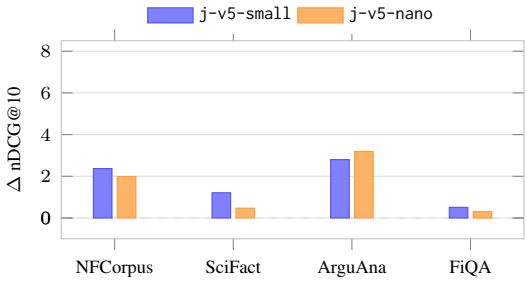

Figure 5: Default SOFTCENTROID (K=3, α=0.5, τ=0.05) on the four headline tasks at full BEIR, showing the three regimes: ArguAna (symmetric) breaks decisively; NFCorpus (medical-IR) bends with moderate gain; SciFact and FiQA (asymmetric) hold near baseline.

gains over ten points on full-BEIR `e5-base-v2` at $p < 0.0001$, as Table 5 reports. The trivial program P_0 is dominated on symmetric retrieval across both embedding-model families. The break is enabled by the symmetry of the task: query and document are drawn from the same distribution, which makes "move $\mathbf{q}$ onto the document manifold" the right operation. The cosine geometry is not abandoned. The program exploits it more aggressively than P_0 does.

The paradigm bends on medical-IR headlines. On NFCorpus, the default SOFTCENTROID program gains +2.0 to +2.4 nDCG@10 with $p < 0.001$, and 67 to 80% of the oracle gain survives validation. The lift is real but bounded. It is large enough to be worth the two extra matrix multiplies and small enough that one cannot say cosine plus single-forward is dominated. The geometry is the same, used with a slightly larger program.

The paradigm holds on QA-leaning asymmetric tasks for the centroid algebra alone, but the fusion lever from Section 5.6 closes much of the gap. The structural reason is that the local top-K document centroid is dominated by lexical-overlap neighbours of the question; estimating "what answers this question" from the document manifold alone is harder than estimating "what is similar." Composing SOFTCENTROID with BM25 fusion flips NQ and HotpotQA from non-positive to positive on `e5-base-v2` nanoBEIR. The QA limitation of pure centroid replacement is thus an addressable boundary rather than a fundamental ceiling.

6 Discussion

Our contribution is not that centroid replacement helps, which is consistent with classical PRF, but the positive separation between document-manifold programs and stochastic ensembling. Among the seventeen substrate families explored, document-manifold programs form a distinct frontier dominating stochastic ensembling on every cell where they fire, with 99% of oracle gain retained on ArguAna under dev/test selection. ArguAna retrieves counter-arguments where query and document are drawn from the same distribution. Replacing $\mathbf{q}$ with the weighted mean of the top documents moves it onto the document manifold, exactly the right place under symmetric retrieval. The K=1 setting that replaces the query with the top-1 document alone gives +6.4 to +7.1 on ArguAna while losing 3 to 4 points on asymmetric SciFact and FiQA.

The agentic loop's contribution is not the algebraic recipe, which is close to known PRF, but the autoresearch artifact. The default K=3, α=0.5, τ=0.05 ports across seven embedding-model families without a per-task hyperparameter sweep, and the long-horizon memory documents which substrate families do not generalize. Rocchio remains a strong simple baseline. The generation loop eliminates grid-search overhead and provides a reusable scaffolding for re-running the search on any embedding model. The parameter sensitivity of this default is visualized in Figure 8 in Appendix D, which shows per-task lift across the α, K, and τ sweeps on `e5-base-v2`.

Practical deployment relies on approximate nearest-neighbour search rather than exact cosine. We measure the lift's robustness to HNSW (Malkov and Yashunin, 2020) parameter variation on `e5-base-v2` NFCorpus. The lift stays within $[+1.44, +1.63]$ across wide sweeps of efSearch, efConstruction, and graph degree M, all significant at $p < 0.01$. Centroid replacement composes with off-the-shelf ANN stacks without parameter-specific tuning. End-to-end latency on the same index is $+0.75$ ms ($+6\%$) on an NVIDIA L4 GPU and $+1.08$ ms ($+2\%$) on CPU, because the encoder forward pass dominates and the second HNSW call plus centroid construction add sub-millisecond overhead.

The pattern across the three regimes is that direct ports of the LLM TTC playbook diverge from the discovered frontier. DROPOUTENS, the best-of-N analogue, sits at baseline. ASYMLORA, which samples under different LoRA conditioning, sits well below baseline because asymmetric LoRA misaligns the query and document subspaces. Generative TTC wins because the output space is discrete and a verifier collapses a noisy distribution to a sharper mode. A dense embedding model's output is a single point on the unit sphere $\mathbb{S}^{d-1}$. Averaging M stochastic embeddings leaves $\mathbb{S}^{d-1}$, and re-normalizing projects onto a Karcher-mean approximation in a metric the embedding model was not trained to respect. There is also no inference-time verifier signal. What works is operations that respect the ranking algebra. Rocchio-style updates keep $\mathbf{q}$ near its trained location and nudge it toward the local centroid the embedding model already considers similar.

Every frontier program leaves the cosine geometry intact and uses extra inference compute to find a better point in it. The adaptive-routing search (Section 4.4) demonstrates that the embedding TTC regime has the same fixed-versus-adaptive separation that characterizes LLM TTC (Snell et al., 2025): the frontier is not yet saturated once routing policy is added to the search space.

This is the empirical ceiling under a frozen single-vector embedding model with no second model and no extra training. Lifting it will require either changing the embedding model, through multi-vector late interaction or trained TTC adapters, or admitting an external generator in the inference path.

A researcher who already knows that Rocchio-style updates are the right direction can define a grid over $(K, \alpha, \tau, \text{anchor})$ and recover SOFTCENTROID in a few hundred evaluations. The loop adds value on three axes that a focused grid cannot. First, the loop explores substrate families the researcher may not anticipate: 259 programs span 17 substrate families, and approximately 170 of those programs are anti-patterns, specifically LoRA fusion, dropout ensembles, dimension gating, and score-space-only methods, whose falsification is itself informative. The long-horizon memory accumulates these ruled-out hypotheses so any future search on a new embedding model can skip structurally equivalent ideas without re-running them. Second, convergence to the centroid family was an emergent finding rather than a preset hypothesis. The loop started with LLM-TTC substrates and discovered centroid replacement after those failed. A focused centroid grid assumes the conclusion. Third, the long-horizon memory is a reusable artifact: dropping in a different embedding model means the agent skips the 170 known anti-patterns immediately, concentrating evaluations on the open hypotheses.

If the productive direction is already known to be pseudo-relevance feedback in embedding space, a focused centroid grid will converge faster than the unsupervised loop. The loop's comparative advantage is hypothesis generation under uncertainty, not parameter optimization once the winning substrate family is known.

The universality criterion's gating set, defined as {NFCorpus, SciFact, ArguAna}, affects which programs are admitted to the frontier. We assess this sensitivity post-hoc using the `e5-base-v2` 13-task nanoBEIR evaluation from Section F. Replacing the gating set with {NFCorpus, FiQA-2018, SciFact} still admits SOFTCENTROID as universal positive (per-task deltas $+0.58$, $+1.66$, $+0.55$). Replacing it with {NQ, HotpotQA, ArguAna} excludes SOFTCENTROID because NQ (-0.42) and HotpotQA (-1.31) are negative under pure centroid replacement; those cells are recovered by the BM25 fusion lever described in Section 5.6. Using all 13 tasks as a strict gating criterion also excludes SOFTCENTROID (8 of 13 positive). The original gating set therefore represents a conservative but achievable coverage criterion that spans medical IR, scientific fact verification, and symmetric retrieval, the three paradigms where pure centroid algebra produces reliable lift. QA-leaning gating sets would have directed the search toward hybrid programs earlier, but such programs were

not fully within the training-free, no-LLM substrate constraint.

The anchor choice for the $2\times$ regime was explored beyond FIRSTSENT. Title-field variants produce strong ArguAna gains but fail to achieve universal-positive status on NFCorpus, because the curated title carries the argument topic on debate corpora but does not reliably signal medical-document relevance where the first sentence of the body carries the clinical framing. FIRSTSENT avoids this task-specificity by extracting the opening of the body rather than the metadata field.

7 Conclusion

The common reading that test-time compute is reserved for large reasoning LLMs does not hold for the class of embedding models distilled from those same LLMs. A frozen single-vector embedding model admits a structured, model-family-agnostic class of test-time interventions whose discovery is the contribution of this paper. The boundary the search exposes is geometric rather than empirical. Stochastic best-of-N aggregators leave the unit sphere and lose the ranking algebra. Structured updates that move the query toward the local document centroid survive across seven embedding-model families at full-BEIR scale, with statistically significant gains on the symmetric and medical-IR headlines and held-out lifts on SCIDOCS and Touche2020. A complementary BM25 score fusion lever stacked on top of SOFTCENTROID broadens the gain across the wider nanoBEIR suite.

The most useful artefact is not the winning program but the rerunnable loop, long-horizon memory, and program registry that produced it. Substituting a different embedding-model family or benchmark will produce a different frontier subject to the same geometric ceiling. The search demonstrates that the frontier is not static: query-adaptive compute routing, which gates on query length and retrieval confidence, universally improves over the fixed SOFTCENTROID default while remaining within the same centroid algebra. The cosine paradigm is not erased by test-time compute, only wrapped. The remaining open question is whether that ceiling can be lifted from inside the cosine paradigm, or only by changing the embedding model.

References

Mohammad Kalim Akram, Saba Sturua, Nastia Havriushenko, Quentin Herreros, Michael Günther, Maximilian Werk, and Han Xiao. 2026. jina-embeddings-v5-text: Task-targeted embedding distillation. *arXiv preprint arXiv:2602.15547*.

Vera Boteva, Demian Gholipour Ghalandari, Artem Sokolov, and Stefan Riezler. 2016. A full-text learning to rank dataset for medical information retrieval. In *Advances in Information Retrieval: 38th European Conference on IR Research (ECIR)*, pages 716–722.

Bradley Brown, Jordan Juravsky, Ryan Ehrlich, Ronald Clark, Quoc V. Le, Christopher Ré, and Azalia Mirhoseini. 2024. Large language monkeys: Scaling inference compute with repeated sampling. *arXiv preprint arXiv:2407.21787*.

Kenneth Enevoldsen, Isaac Chung, Imene Kerboua, Márton Kardos, Ashwin Mathur, David Stap, Jay Gala, Wissam Siblini, Dominik Krzemiński, Genta Indra Winata, and 1 others. 2025. MMTEB: Massive multilingual text embedding benchmark. In *The Thirteenth International Conference on Learning Representations (ICLR)*. ArXiv:2502.13595.

Thibault Formal, Benjamin Piwowarski, and Stéphane Clinchant. 2021. SPLADE: Sparse lexical and expansion model for first stage ranking. In *Proceedings of the 44th International ACM SIGIR Conference on Research and Development in Information Retrieval (SIGIR)*, pages 2288–2292.

Luyu Gao, Xueguang Ma, Jimmy Lin, and Jamie Callan. 2023. Precise zero-shot dense retrieval without relevance labels. In *Proceedings of the 61st Annual Meeting of the Association for Computational Linguistics (Volume 1: Long Papers)*, pages 1762–1777.

Omar Khattab and Matei Zaharia. 2020. ColBERT: Efficient and effective passage search via contextualized late interaction over BERT. In *Proceedings of the 43rd International ACM SIGIR Conference on Research and Development in Information Retrieval (SIGIR)*, pages 39–48.

Victor Lavrenko and W. Bruce Croft. 2001. Relevance-based language models. In *Proceedings of the 24th Annual International ACM SIGIR Conference on Research and Development in Information Retrieval (SIGIR)*, pages 120–127.

Chankyu Lee, Rajarshi Roy, Mengjie Xu, Jonathan Raiman, Mohammad Shoeybi, Bryan Catanzaro, and Wei Ho. 2025. NV-Embed: Improved techniques for training LLMs as generalist embedding models. In *The Thirteenth International Conference on Learning Representations (ICLR)*. ArXiv:2405.17428.

Joel Lehman, Jonathan Gordon, Shawn Jain, Kamal Ndousse, Cathy Yeh, and Kenneth O. Stanley. 2024. Evolution through large models. In Wolfgang Banzhaf, Penousal Machado, and Mengjie Zhang, editors, *Handbook of Evolutionary Machine Learning*, Genetic and Evolutionary Computation. Springer.

Hang Li, Ahmed Mourad, Shengyao Zhuang, Bevan Koopman, and Guido Zuccon. 2023a. Pseudo relevance feedback with deep language models and dense retrievers: Successes and pitfalls. *ACM Transactions on Information Systems*, 41(3):1–40.

Hang Li, Xiao Wang, Bevan Koopman, and Guido Zuccon. 2025a. Pseudo relevance feedback is enough to close the gap between small and large dense retrieval models. *arXiv preprint arXiv:2503.14887*.

Hang Li, Shengyao Zhuang, Bevan Koopman, and Guido Zuccon. 2025b. LLM-VPRF: Large language model based vector pseudo relevance feedback. *arXiv preprint arXiv:2504.01448*.

Zehan Li, Xin Zhang, Yanzhao Zhang, Dingkun Long, Pengjun Xie, and Meishan Zhang. 2023b. Towards general text embeddings with multi-stage contrastive learning. *arXiv preprint arXiv:2308.03281*.

Macedo Maia, Siegfried Handschuh, André Freitas, Brian Davis, Ross McDermott, Manel Zarrouk, and Alexandra Balahur. 2018. WWW'18 open challenge: Financial opinion mining and question answering. In *Companion Proceedings of The Web Conference 2018*, pages 1941–1942.

Yu A. Malkov and Dmitry A. Yashunin. 2020. Efficient and robust approximate nearest neighbor search using hierarchical navigable small world graphs. *IEEE Transactions on Pattern Analysis and Machine Intelligence*, 42(4):824–836.

Rui Meng, Ye Liu, Semih Yavuz, Rishabh Agarwal, Lifu Tu, Ning Yu, Jiacheng Zhang, Zhengdong Chen, and Hetal Raghavan. 2024. SFR-Embedding-2: Advanced text embeddings with multi-stage training. Salesforce AI Research. `https://huggingface.co/Salesforce/SFR-Embedding-2_R`.

Niklas Muennighoff, Hongjin Su, Liang Wang, Nan Yang, Furu Wei, and Tao Shi. 2025. Generative representational instruction tuning. In *The Thirteenth International Conference on Learning Representations (ICLR)*. ArXiv:2402.09906.

Niklas Muennighoff, Nouamane Tazi, Loic Magne, and Nils Reimers. 2023. MTEB: Massive text embedding benchmark. In *Proceedings of the 17th Conference of the European Chapter of the Association for Computational Linguistics (EACL)*, pages 2014–2037.

Shahrzad Naseri, Jeffrey Dalton, Andrew Yates, and James Allan. 2021. CEQE: Contextualized embeddings for query expansion. In *Advances in Information Retrieval: 43rd European Conference on IR Research (ECIR)*, pages 467–482.

Alexander Novikov, Ngân Vũ, Marvin Eisenberger, Emilien Dupont, Po-Sen Huang, Adam Zsolt Wagner, Sergey Shirobokov, Borislav Kozlovskii, Francisco J. R. Ruiz, Abbas Mehrabian, M. Pawan Kumar, Abigail See, Swarat Chaudhuri, George Holland, Alex Davies, Sebastian Nowozin, Pushmeet Kohli, and Matej Balog. 2025. AlphaEvolve: A coding agent for scientific and algorithmic discovery. *arXiv preprint arXiv:2506.13131*.

Stephen E. Robertson, Steve Walker, Susan Jones, Micheline M. Hancock-Beaulieu, and Mike Gatford. 1995. Okapi at TREC-3. In *Proceedings of the Third Text REtrieval Conference (TREC-3), NIST Special Publication 500-225*, pages 109–126. National Institute of Standards and Technology.

Joseph J. Rocchio. 1971. Relevance feedback in information retrieval. In Gerard Salton, editor, *The SMART Retrieval System: Experiments in Automatic Document Processing*, pages 313–323. Prentice-Hall, Englewood Cliffs, NJ.

Bernardino Romera-Paredes, Mohammadamin Barekatain, Alexander Novikov, Matej Balog, M. Pawan Kumar, Emilien Dupont, Francisco J. R. Ruiz, Jordan S. Ellenberg, Pengming Wang, Omar Fawzi, Pushmeet Kohli, and Alhussein Fawzi. 2024. Mathematical discoveries from program search with large language models. *Nature*, 625(7995):468–475.

Keshav Santhanam, Omar Khattab, Jon Saad-Falcon, Christopher Potts, and Matei Zaharia. 2022. ColBERTv2: Effective and efficient retrieval via lightweight late interaction. In *Proceedings of the 2022 Conference of the North American Chapter of the Association for Computational Linguistics: Human Language Technologies (NAACL-HLT)*, pages 3715–3734.

Charlie Snell, Jaehoon Lee, Kelvin Xu, and Aviral Kumar. 2025. Scaling LLM test-time compute optimally can be more effective than scaling parameters for reasoning. In *The Thirteenth International Conference on Learning Representations (ICLR)*. ArXiv:2408.03314.

Nandan Thakur, Nils Reimers, Andreas Rücklé, Abhishek Srivastava, and Iryna Gurevych. 2021. BEIR: A heterogeneous benchmark for zero-shot evaluation of information retrieval models. In *Proceedings of the Neural Information Processing Systems Track on Datasets and Benchmarks*.

Yiteng Tu, Weihang Su, Yujia Zhou, Yiqun Liu, Fen Lin, Qin Liu, and Qingyao Ai. 2026. Generalized pseudo-relevance feedback. In *Proceedings of the ACM Web Conference 2026 (WWW '26)*, pages 1876–1886. ArXiv:2510.25488.

Omri Uzan, Asaf Yehudai, Roi Pony, Eyal Shnarch, and Ariel Gera. 2026. Guided query refinement: Multimodal hybrid retrieval with test-time optimization. In *The Fourteenth International Conference on Learning Representations (ICLR)*. ArXiv:2510.05038.

Henrique Schechter Vera, Sahil Dua Salz, Po-Sen Suganthan, Dan Iter, Yichang Naim, Jan Botha, Yury Choe, Sanjiv Mukherjee, Varun Kishore, Kunal Singhal, Iftekhar Naim, Eduard Hovy, Sherry Yan, and 1 others. 2025. EmbeddingGemma: Powerful and lightweight text representations. *arXiv preprint arXiv:2509.20354*.

Henning Wachsmuth, Shahbaz Syed, and Benno Stein. 2018. Retrieval of the best counterargument without prior topic knowledge. In *Proceedings of the 56th Annual Meeting of the Association for Computational Linguistics (Volume 1: Long Papers)*, pages 241–251.

David Wadden, Shanchuan Lin, Kyle Lo, Lucy Lu Wang, Madeleine van Zuylen, Arman Cohan, and Hannaneh Hajishirzi. 2020. Fact or fiction: Verifying scientific claims. In *Proceedings of the 2020 Conference on Empirical Methods in Natural Language Processing (EMNLP)*, pages 7534–7550.

Liang Wang, Nan Yang, Xiaolong Huang, Binxing Jiao, Linjun Yang, Daxin Jiang, Rangan Majumder, and Furu Wei. 2022. Text embeddings by weakly-supervised contrastive pre-training. *arXiv preprint arXiv:2212.03533*.

Liang Wang, Nan Yang, and Furu Wei. 2023a. Query2doc: Query expansion with large language models. In *Proceedings of the 2023 Conference on Empirical Methods in Natural Language Processing (EMNLP)*, pages 9414–9423.

Xuezhi Wang, Jason Wei, Dale Schuurmans, Quoc V. Le, Ed H. Chi, Sharan Narang, Aakanksha Chowdhery, and Denny Zhou. 2023b. Self-consistency improves chain of thought reasoning in language models. In *The Eleventh International Conference on Learning Representations (ICLR)*.

Yangzhen Wu, Zhiqing Sun, Shanda Li, Sean Welleck, and Yiming Yang. 2025. Inference scaling laws: An empirical analysis of compute-optimal inference for problem-solving with language models. In *The Thirteenth International Conference on Learning Representations (ICLR)*. ArXiv:2408.00724.

Zilin Xiao, Qi Ma, Mengting Gu, Chun-cheng Jason Chen, Xintao Chen, Vicente Ordonez, and Vijai Mohan. 2026. MetaEmbed: Scaling multimodal retrieval at test-time with flexible late interaction. In *The Fourteenth International Conference on Learning Representations (ICLR)*. ArXiv:2509.18095; Oral.

HongChien Yu, Chenyan Xiong, and Jamie Callan. 2021. Improving query representations for dense retrieval with pseudo relevance feedback. In *Proceedings of the 30th ACM International Conference on Information & Knowledge Management (CIKM)*, pages 3592–3596.

Zeta Alpha. 2024. Nanobeir: A lightweight benchmark for information retrieval evaluation. `https://huggingface.co/collections/zeta-alpha-ai/nanobeir-66e1a0af21dfd93e620cd9f6`. Accessed 2026.

Yanzhao Zhang, Mingxin Li, Dingkun Long, Xin Zhang, Huan Lin, Baosong Yang, Pengjun Xie, An Yang, Dayiheng Liu, Junyang Lin, Fei Huang, and Jingren Zhou. 2025. Qwen3 Embedding: Advancing text embedding and reranking through foundation models. *arXiv preprint arXiv:2506.05176*.

Shengyao Zhuang, Xueguang Ma, Bevan Koopman, Jimmy Lin, and Guido Zuccon. 2024. PromptReps: Prompting large language models to generate dense and sparse representations for zero-shot document retrieval. In *Proceedings of the 2024 Conference on Empirical Methods in Natural Language Processing (EMNLP)*, pages 4375–4391.

A Baseline Reproduction

Model	Task	Pub.	Ours	Δ
`j-v5-small`	NFCorpus	39.81	39.76	-0.05
	SciFact	76.53	76.59	$+0.06$
	ArguAna	65.07	64.71	-0.36
	FiQA-2018	49.63	49.52	-0.11
`j-v5-nano`	NFCorpus	38.69	38.75	$+0.07$
	SciFact	75.78	75.91	$+0.13$
	ArguAna	65.70	65.63	-0.07
	FiQA-2018	47.85	47.87	$+0.02$

Table 10: Reproduction of the trivial program P_0, the cosine baseline with single forward pass, reporting nDCG@10 $\times 100$ for `j-v5-small` and `j-v5-nano` on four BEIR tasks. "Pub." is the published leaderboard number and "Ours" is our fp16 reproduction. All eight cells lie within 0.4 nDCG points.

B Cost-Accuracy Pareto Frontier and Test-Time Scaling

Table 11 aggregates the 1,522 program-task evaluations across the registry. At each cost stratum it reports the best mean Δ nDCG@10, averaged across the four BEIR tasks, any program achieved. The frontier rises sharply from $1\times$ to $2\times$, gaining $+2.65$, and saturates at $+2.67$ near 3 to $4\times$. At 5 to $9\times$ the best mean drops to $+2.51$ as multi-LoRA gates introduce misaligned anchors. The maximum true TTC cost in the registry is $9\times$. The empirical scaling is qualitatively distinct from the log-linear best-of-N curve reported for generative TTC (Brown et al., 2024). Dense-retrieval test-time compute is concave and bounded by the geometric ceiling of the cosine paradigm.

A complementary form of test-time scaling, internal to the centroid algebra itself, is to iterate SoftCentroid multiple times on the same encoded query. On full-BEIR ArguAna, where the dense baseline is far from the document manifold, iterating the centroid update lifts the result further on every model tested, as Table 12 reports. The single-iteration default already yields lifts ranging from $+3.56$ on `gte-base-en-v1.5` to $+12.55$ on `e5-base-v2` at $p < 10^{-4}$. Iterating to the model-specific peak between iters two and five adds a fur-

Cost stratum	# programs	Best mean Δ	Best max Δ
1×	14	+2.56	+7.13
2×	71	+2.65	+7.18
3× – 4×	133	**+2.67**	+7.13
5× – 9×	22	+2.51	+7.10

Table 11: Test-time scaling on the four BEIR tasks NFCorpus, SciFact, ArguAna, and FiQA, across both `j-v5-small` and `j-v5-nano`. "Best mean Δ" is the highest mean Δ nDCG@10 (×100) any program achieved across the eight cells at that cost stratum. The frontier saturates between 2× and 4× cost. The gain from 1× to 2× is +2.62, from 2× to 4× is +0.05, and beyond 4× is negative or null.

ther +0.91 to +3.18 nDCG@10 at $p < 10^{-4}$ on all seven models. Extending the grid on `e5-base-v2` to twenty iterations confirms a clear peak rather than unbounded growth, as Figure 6 shows. The lift saturates at +15.73 at iter 5, decays gently to +15.26, +14.74, +14.22, and +14.01 at iters 7, 10, 15, 20, and remains statistically significant at $p < 10^{-4}$ throughout.

ArguAna therefore admits deeper test-time scaling within the discovered algebraic family across the entire embedding-model family, not just one. We retain the single-iteration default in the main results because the universality criterion of Section 3 requires non-negativity across the full task spectrum, and iteration-budget transfer is itself task-dependent. The pattern reproduces on held-out SCIDOCS at full-BEIR scale with `e5-base-v2`. Iter 1 peaks at +0.54 at p=0.016 and the lift decays through iters 2, 3, 4, 5 to +0.46 ns, +0.21, +0.12, +0.10. This confirms that the iteration axis is not held-out-restricted but rather task-restricted, with single-step updates serving as the safe default outside ArguAna-like manifolds.

The two paper-level levers compose orthogonally. Stacking BM25 fusion from Section 5.6 on iterative SOFTCENTROID for `e5-base-v2` elevates the iteration trajectory across all three medical-IR and finance-IR headlines tested. On NFCorpus, fusion lifts the iter-one, two, and three deltas from +1.11, +0.41, −0.06 under pure SC to +1.79, +1.60, +1.62, with $p \leq 0.015$ on every fused cell. Pure SC on the same model loses significance after iter one. The same fusion lever moves SciFact's three deltas from +0.25, −0.49, −1.46 to +1.10, +0.41, −0.32, and FiQA-2018's from +0.01, −1.07, −1.54 to +1.73 at p=0.004, then +0.73, then −0.17. The lexical signal therefore stabilizes the centroid update across iterations rather than adding a constant offset. On the three tasks tested, every iter-one fused cell either stays in or moves into positive territory.

The same stabilization holds across embedding-model families. On NFCorpus, fusion lifts the iter-one through iter-three trajectory into statistical significance at $p < 0.05$ on every cell of `e5-small-v2`, `e5-base-v2`, `e5-large-v2`, and `gte-base-en-v1.5`, with deltas ranging from +1.39 to +2.60 at iter two when pure SC on the same models has already lost significance on three of four. The two task-LoRA `j-v5-small` and `j-v5-nano` headline models show the same pattern. Fusion holds iter three at +1.66* on `j-v5-small` where pure SC sits at +0.96 ns, and elevates iter two to +1.86* on `j-v5-nano` where pure SC sits at +1.21 ns. A controlled iteration-budget schedule that tightens the centroid pull when the local manifold is symmetric and freezes after one step otherwise is a productive direction for future work, but lies outside the program family explored by the present search.

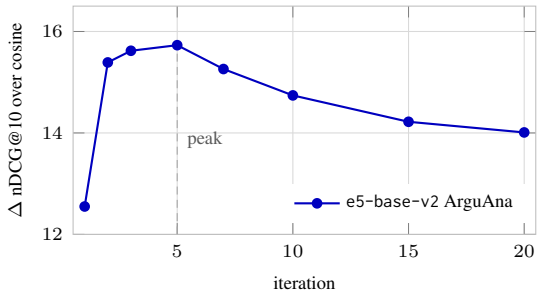

Figure 6: Iterative SOFTCENTROID on `e5-base-v2` full-BEIR ArguAna across twenty iterations. The lift saturates at iter 5 at +15.73 nDCG@10 and decays gently afterwards, remaining statistically significant at $p < 10^{-4}$ throughout the range.

C Held-Out Cross-Model Validation

Table 13 consolidates the held-out full-BEIR evidence reported inline in Section 5, and Figure 7 visualises the eight cells. SCIDOCS uses 1,000 queries and a 25,657-document corpus with multi-relevance labels, averaging around 30 gold documents per query. Touche2020 uses 49 queries on a 25,000-document subsample that preserves all 2,099 gold documents in a BM25-favorable argumentation domain. Both tasks were strictly held out from the agentic loop's frontier-admission gate. The table reports paired-bootstrap Δ nDCG@10 with 10,000 resamples on per-query nDCG@10. The mean fusion lift across the eight held-out cells

Encoder (params)	iter 1	iter 2	iter 3	iter 5
`e5-small-v2` (33M)	+9.47	+10.97	+11.20	+10.51
`e5-base-v2` (110M)	+12.55	+15.39	+15.62	+15.73
`e5-large-v2` (335M)	+10.27	+11.57	+11.46	+11.00
`gte-base-en-v1.5` (110M)	+3.56	+4.47	+4.08	+4.24
`bge-large-en-v1.5` (335M)	+5.03	+6.29	+6.39	+6.30
`j-v5-small`	+4.74	+6.20	+6.43	+6.19
`j-v5-nano`	+5.64	+7.01	+7.37	+7.00

Table 12: Iterative SOFTCENTROID on full-BEIR ArguAna, reporting Δ nDCG@10 ($\times 100$) versus the cosine baseline at iterations one, two, three, and five. Every cell is statistically significant at $p < 10^{-4}$ on a paired bootstrap with 10,000 resamples. All seven models peak between iterations two and five, with peak gains exceeding the single-iteration default by $+0.91$ to $+3.18$ nDCG@10.

is $+3.31$ over the dense baseline and $+4.42$ over pure SOFTCENTROID.

D SOFTCENTROID Hyperparameter Ablation

Table 15 reports the one-parameter ablation around the recommended default $K{=}3, \alpha{=}0.5, \tau{=}0.05$ on `j-v5-small` and `j-v5-nano`. Interpolation α and softmax temperature τ carry most of the gain. Centroid size K is largely inert across $K \in \{3, 5, 8\}$. On `e5-base-v2`, the same one-parameter sweep at full-BEIR scale reproduces the `j-v5` pattern and surfaces the same task-specific asymmetry seen for iterative SOFTCENTROID in Section B. NFCorpus has a clear stable region around the default, with $\alpha \in [0.2, 0.5]$ at $p < 0.01$, $\tau \in \{0.02, 0.05\}$ at $p \leq 0.02$, and $K \in \{2, 3\}$ at $p < 0.01$. ArguAna scales monotonically along every axis.

Figure 8 visualizes the full α, K, and τ sweeps on `e5-base-v2` as heat maps. Each cell encodes Δ nDCG@10 ($\times 100$) versus the cosine baseline, with the paper default (bold border) sitting in a clear positive region on NFCorpus and exhibiting monotonic improvement on ArguAna. The FiQA-2018 and SciFact panels confirm that most parameter choices produce near-zero or slightly positive delta on those tasks; the slight negative values at large K and large τ on SciFact are not statistically significant. The visualization makes the task-asymmetry story immediate: any $\alpha \geq 0.2$, any $K \leq 5$, and any $\tau \leq 0.05$ sustains the NFCorpus lift, while ArguAna rewards pushing every parameter toward its extreme.

The ArguAna monotonicity replicates across the full seven-model cohort on every aggressive direction, namely smaller τ, larger α, and smaller K, as Table 14 reports. Combined with the iterative-SC peak at iter five from Section B, ArguAna admits deeper test-time intervention on four independent axes across embedding-model families, with 77 of 77 aggressive-direction cells significant at $p < 10^{-4}$. Every model gains by sharpening the centroid through smaller τ and smaller K, and by giving more weight to the centroid in the interpolation through larger α. This is consistent with the symmetric-retrieval geometry in which the document and query manifolds coincide. The universal default is the conservative pick that survives the cross-task universality criterion of Section 3. The asymmetric admission of more aggressive parameters on ArguAna is the same geometric story.

E Extended Baseline Comparisons

Table 16 compares SOFTCENTROID against four families of training-free alternatives under the same frozen-encoder regime. All methods use $K{=}3$ and $\alpha{=}0.5$ to match the SOFTCENTROID default. Mean Δ nDCG@10 ($\times 100$) is averaged across three encoder families (`e5-base-v2`, `j-v5-small`, `bge-large-en-v1.5`).

The hard top-1 variant (replacing the query with the single nearest document embedding) deserves comment: it is the $\alpha{=}1.0, K{=}1$ limit of SOFTCENTROID and was independently discovered by the agentic loop as the PSEUDODOC substrate in early generations (see Section 4). Its strong ArguAna result exploits the symmetric argument-counterargument structure of that task, while the regressions on SciFact and FiQA confirm the task-specificity documented in the long-horizon memory. The SOFTCENTROID default at $K{=}3$ with softmax weighting represents the robust middle ground that generalizes across tasks.

Task	Encoder	baseline	SC Δ	Fusion Δ vs base	Fusion Δ vs SC
SCIDOCS	`e5-base-v2`	0.186	$+0.54^{*}$	$+1.17^{\ddagger}$	$+0.63^{\dagger}$
SCIDOCS	`e5-large-v2`	0.206	$+0.77^{\ddagger}$	$+0.81^{\ddagger}$	$+0.05$
SCIDOCS	`gte-base-en-v1.5`	0.231	$+0.87^{\ddagger}$	$+1.12^{\ddagger}$	$+0.25$
SCIDOCS	`bge-large-en-v1.5`	0.209	$+0.88^{\ddagger}$	$+2.42^{\ddagger}$	$+1.54^{\ddagger}$
Touche2020	`e5-base-v2`	0.529	-1.12	$+4.93^{\dagger}$	$+6.05^{\ddagger}$
Touche2020	`e5-large-v2`	0.481	-0.33	$+5.86^{\ddagger}$	$+6.19^{\ddagger}$
Touche2020	`gte-base-en-v1.5`	0.520	-1.80	$+5.28^{\ddagger}$	$+7.08^{\ddagger}$
Touche2020	`bge-large-en-v1.5`	0.493	-0.77	$+4.91^{\ddagger}$	$+5.68^{\ddagger}$
Mean across 8 held-out cells		—	-0.11	$\mathbf{+3.31}$	$\mathbf{+4.42}$

Table 13: Held-out full-BEIR cross-model validation, reporting Δ nDCG@10 (×100) versus the cosine baseline. The SOFTCENTROID default uses K=3, α=0.5, τ=0.05. Fusion uses BM25 score-level mix at w=0.1, defined in Section 5.6. Significance: ‡ $p < 10^{-3}$, † $p < 10^{-2}$, * $p < 5 \cdot 10^{-2}$ on a paired bootstrap with 10,000 resamples on per-query nDCG@10. All four models on SCIDOCS show stat-sig SOFTCENTROID default lift, with $p \leq 0.001$ on three of four. On Touche2020 the fusion lever provides $p < 10^{-3}$ compensatory lift on all four models. SCIDOCS is multi-relevance scientific IR where the centroid update directly captures relevance. Touche2020 is argument retrieval where dense baselines trail BM25 and the fusion lever provides compensatory lexical signal.

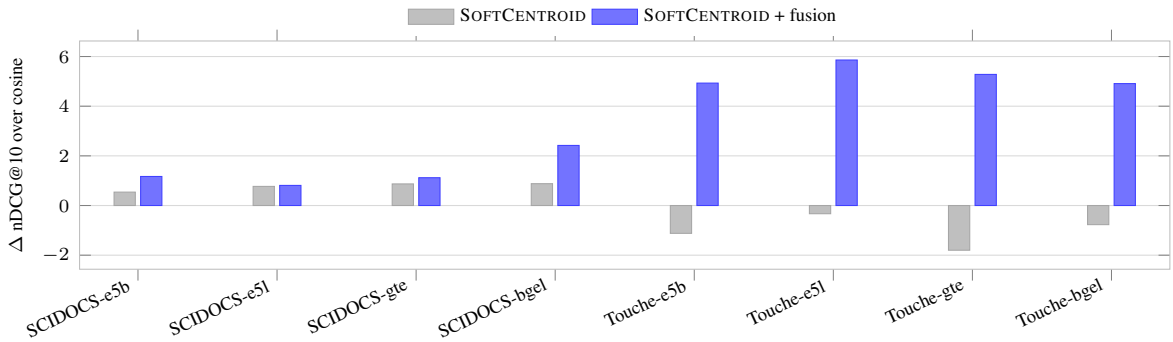

Figure 7: Held-out full-BEIR validation across the eight model-task cells in Table 13. SCIDOCS rewards the centroid lever directly. Touche2020 favours BM25, and the score-fusion lever recovers the lift on every embedding model.

F Cross-Model Transfer Details

F.1 13-Task nanoBEIR Transfer

The model-specificity pattern observed at the headline scale also appears across the broader 13-task nanoBEIR suite. Table 17 applies three frontier SOFTCENTROID variants from the `j-v5` search to `e5-base-v2` across all 13 nanoBEIR retrieval tasks at the 50-query sub-sample. The K=10 variant emerges as the strongest default on this monolithic embedding model.

F.2 4-Task nanoBEIR Probe

Table 18 compares three SOFTCENTROID variants on three monolithic embedding models `e5-base-v2`, `bge-base-en-v1.5`, and `bge-small-en-v1.5` across the four headline BEIR tasks at the 50-query nanoBEIR slice. `e5-base-v2` surfaces as the strongest of the three and was selected for the full-BEIR validation in Table 5.

G Program Flowcharts

Sixteen representative embedding programs from the agent's registry are rendered as flow diagrams. Each diagram shows the sequence of encode, retrieve, aggregate, interpolate, and rerank operations the program executes at inference. The programs span the centroid, anchor, gating, and multi-LoRA substrates explored over ninety generations. Collectively they trace the convergence of the discovered algebra.

H Limitations and Scope

The agent is itself an LLM and inherits whatever priors the underlying model encodes about which substrates are worth exploring. The explicit long-horizon memory and the dev/test paired-bootstrap protocol partially mitigate this, but agent bias can-

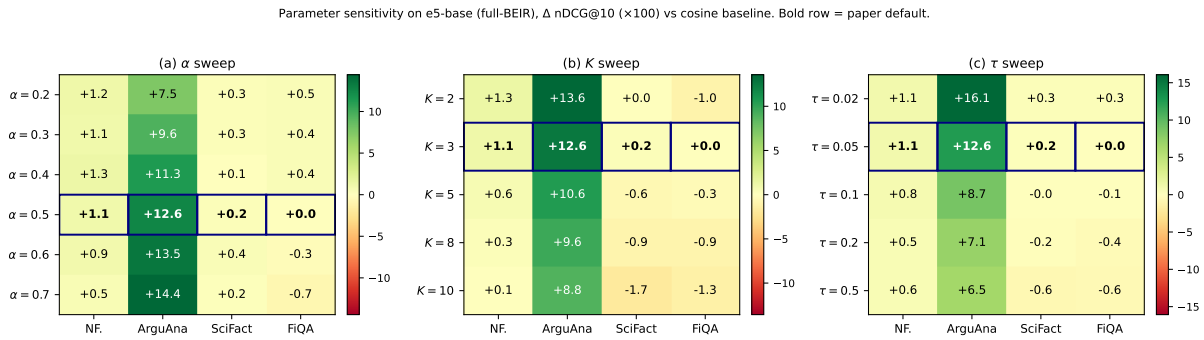

Figure 8: Parameter sensitivity of SoftCentroid on `e5-base-v2` full-BEIR, showing Δ nDCG@10 ($\times 100$) over the cosine baseline for each parameter value across four tasks (NFCorpus, ArguAna, SciFact, FiQA-2018). The paper default is indicated by a navy border. Green cells are positive lifts; red cells are regressions. (a) α sweep (K=3, τ=0.05): NFCorpus is stable for $\alpha \in [0.2, 0.5]$; ArguAna scales monotonically. (b) K sweep (α=0.5, τ=0.05): smaller K is better on NFCorpus and ArguAna; large K introduces regressions on SciFact. (c) τ sweep (K=3, α=0.5): low τ gives the sharpest centroid and the largest ArguAna lift.

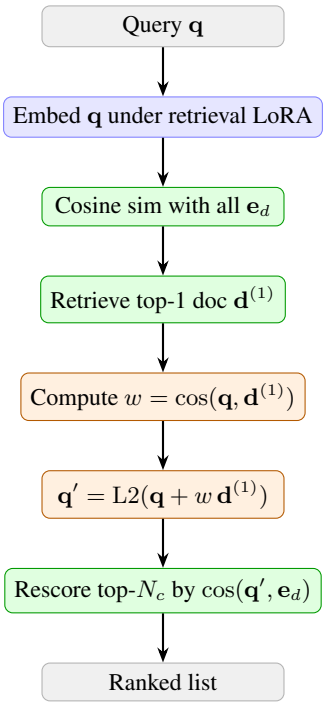

Figure 9: Program P1 (top-1 self-amplification). Encodes query and document under the retrieval LoRA, finds the top-1 document by cosine similarity, then updates the query as $\mathbf{q}' = \mathrm{L2}(\mathbf{q} + w\,\mathbf{d}^{(1)})$ with $w = \cos(\mathbf{q}, \mathbf{d}^{(1)})$, and reranks. The minimal embedding-space PRF and founder of the AMP family. Cost $1\times$.

not be eliminated. A different agent could traverse the embedding-program space differently. The generation loop is a heuristic search and offers no coverage or optimality guarantee. The long-horizon memory reduces redundant exploration but does not certify that the discovered frontier is globally optimal.

Headline experiments use `j-v5-small` and `j-v5-nano`. Full-BEIR cross-model validation extends to `e5-small-v2`, `e5-base-v2`, `e5-large-v2`, `gte-base-en-v1.5`, and `bge-large-en-v1.5` for the fusion lever, as Table 8 shows. For iterative SoftCentroid on ArguAna and the Rocchio comparison, the same five models together with `j-v5-small` and `j-v5-nano` make up the seven-model cohort summarized in Tables 12 and 6. The optimal cluster size K is model-specific. `bge-base-en-v1.5` is partial and `bge-small-en-v1.5` marks the parameter-scale boundary. The algebra is most reliable on models at or above one hundred million parameters. The multi-LoRA adapter design

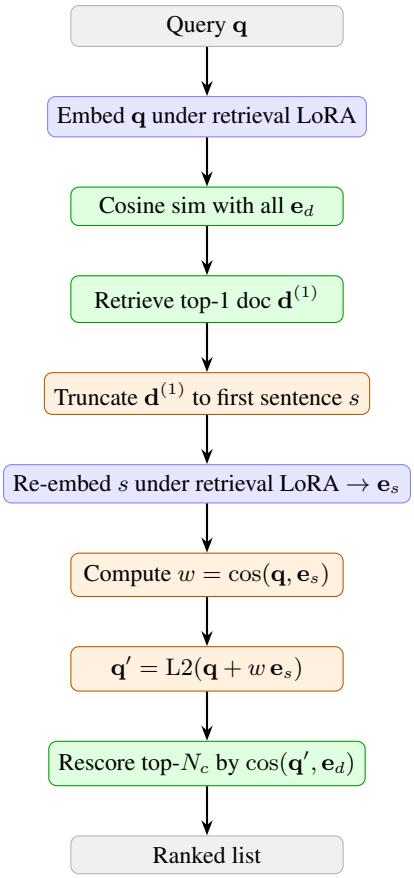

Figure 10: Program P19 (first-sentence anchor). Same skeleton as P1, but the top-1 document is truncated to its first sentence and re-encoded. The resulting first-sentence vector replaces the document anchor. The 2×-cost frontier holder on ArguAna among `j-v5` programs.

Encoder	τ=0.02	α=0.7	K=2
`e5-small-v2`	+14.11	+10.47	+11.07
`e5-base-v2`	+16.07	+14.42	+13.57
`e5-large-v2`	+13.21	+11.16	+10.56
`gte-base-en-v1.5`	+5.50	+4.30	+3.77
`bge-large-en-v1.5`	+5.27	+5.96	+5.18
`j-v5-small`	+5.06	+6.06	+4.92
`j-v5-nano`	+5.77	+6.51	+5.67

Table 14: Aggressive-direction lifts on full-BEIR ArguAna for the seven-model cohort. Every cell is the Δ nDCG@10 ($\times$100) versus the cosine baseline at the listed parameter, with the other parameters fixed at the default K=3, α=0.5, τ=0.05. All 21 cells listed are statistically significant at $p < 10^{-4}$ on a paired bootstrap with 10,000 resamples. The 7 default cells appear in the iter-one column of Table 12. Smaller τ, smaller K, and larger α all monotonically improve nDCG@10 on every model.

of `j-v5` also enables substrate families such as LoRAFusion and AsymLoRA that do not apply to monolithic embedding models, so those specific anti-patterns may not generalize. We evaluate on English BEIR. Performance on multilingual, conversational, or code-retrieval benchmarks is unknown.

The 50-query nanoBEIR slices carry sub-sample variance; we recommend full-BEIR validation before deploying any specific configuration.

Future work can extend the registry by integrating LLM-assisted methods such as HyDE (Gao et al., 2023), LLM-VPRF (Li et al., 2025b), and GPRF (Tu et al., 2026), alongside trained dense-PRF such as ANCE-PRF (Yu et al., 2021), as separate agents in the loop; each occupies a different inference regime than the training-free, no-LLM substrate explored here.

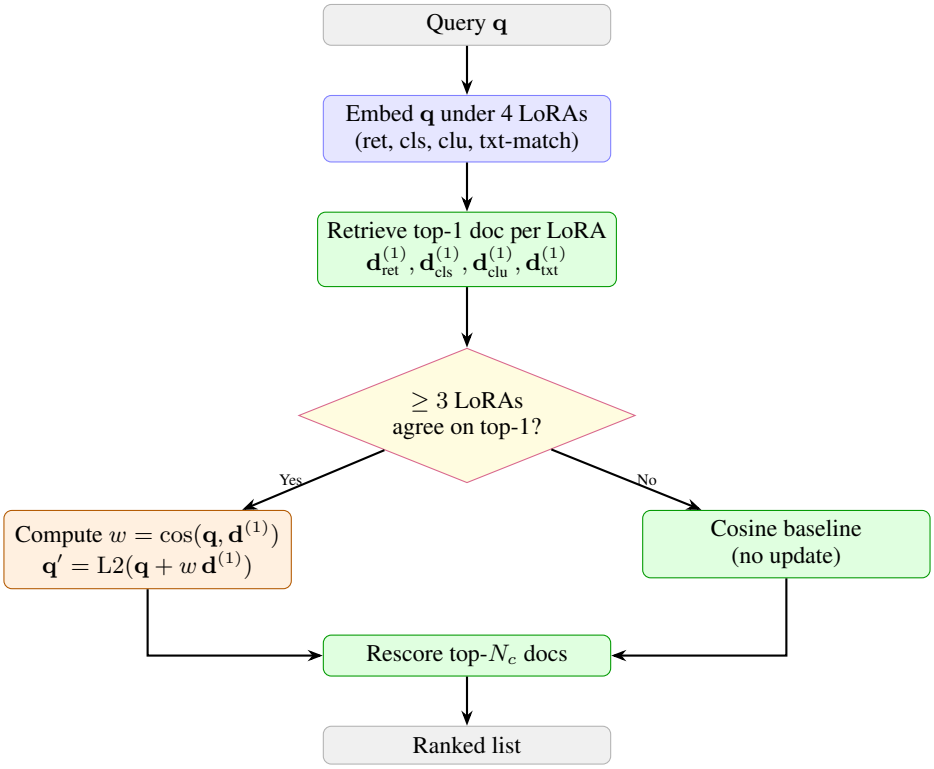

Figure 11: Program P22 (four-LoRA majority gate). Re-encodes the query under all four task-specialized adapters for retrieval, classification, clustering, and text-matching and admits the amp only if at least three LoRAs agree on top-1. A representative LoRAFusion-substrate program. It does not enter the universal frontier because hard-vote over heterogeneous LoRAs averages away the signal that any single LoRA carries.

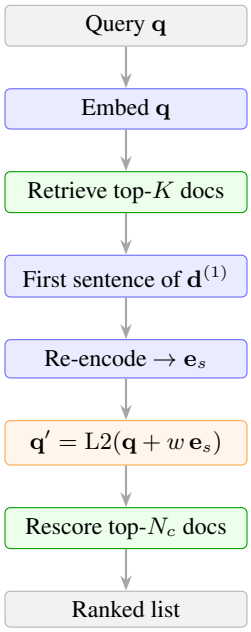

Figure 12: Program P24 (NFCorpus first-sentence variant). An early NFCorpus-tuned member of the AMP family at $3\times$ cost. It was the first to register a positive nano-NFCorpus delta of $+1.20$ nDCG@10 $\times 100$ before the loop generalized to universality.

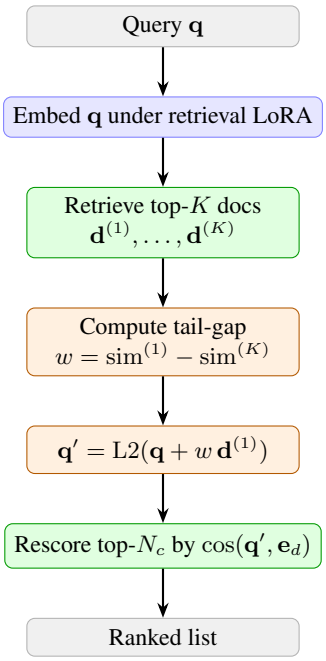

Figure 13: Program P32 (tail-gap weighted amp). Replaces the cosine weight in P1 with a similarity-tail gap $w = \mathrm{sim}^{(1)} - \mathrm{sim}^{(K)}$, so amplification scales with the confidence margin between top-1 and the rest of the top-K. Member of the centroid family.

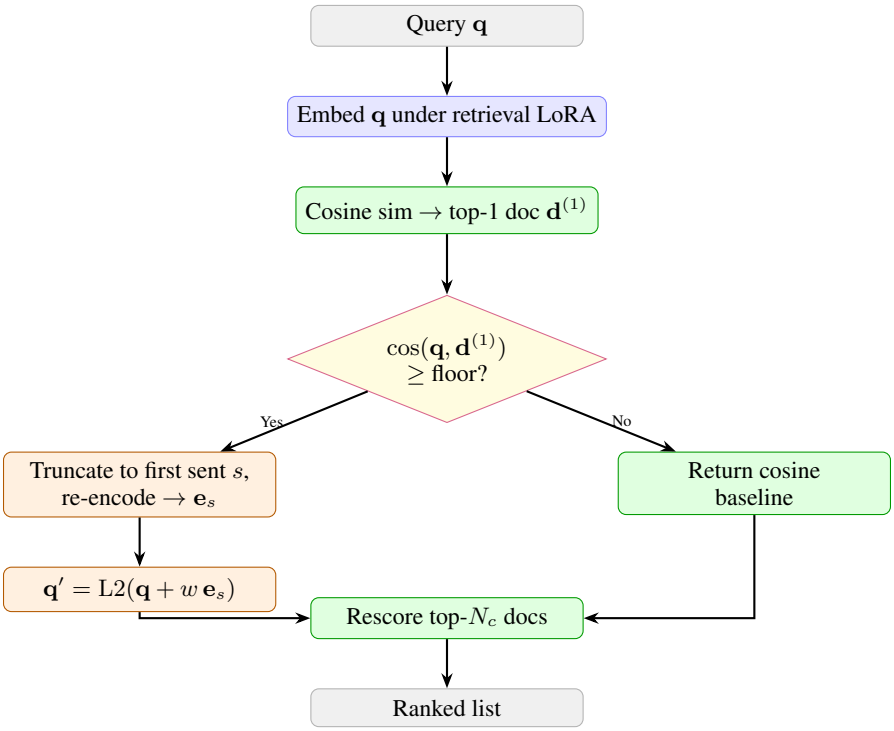

Figure 14: Program P33 (similarity-floor first-sent amp). Adds a lower bound on cosine before the amp fires. Below the floor the program returns the cosine baseline. An early gating-axis exploration that established the gap-confidence pattern reused by later universal champions.

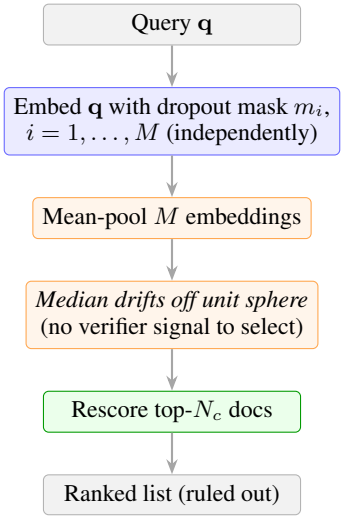

Figure 15: Program P35, the DROPOUTENS stochastic dropout ensemble. Encodes the query M times under independent dropout masks, mean-pools the resulting embeddings, and reranks. Direct port of the LLM best-of-N recipe. Ruled out because the median of unit-norm embeddings leaves the unit sphere and there is no verifier signal to select among samples.

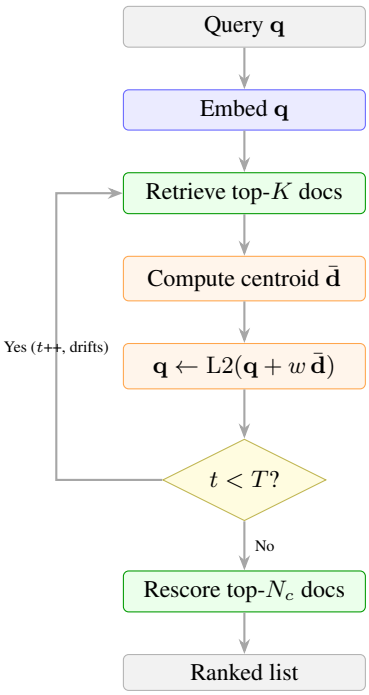

Figure 16: Program P40 (multi-round Rocchio). Iterates the centroid update for $T > 1$ rounds, re-retrieving after each query update. Ruled out: rounds beyond $T = 1$ drift the query off the document manifold and lose ranking accuracy. The search moved beyond the multi-round-PRF substrate early.

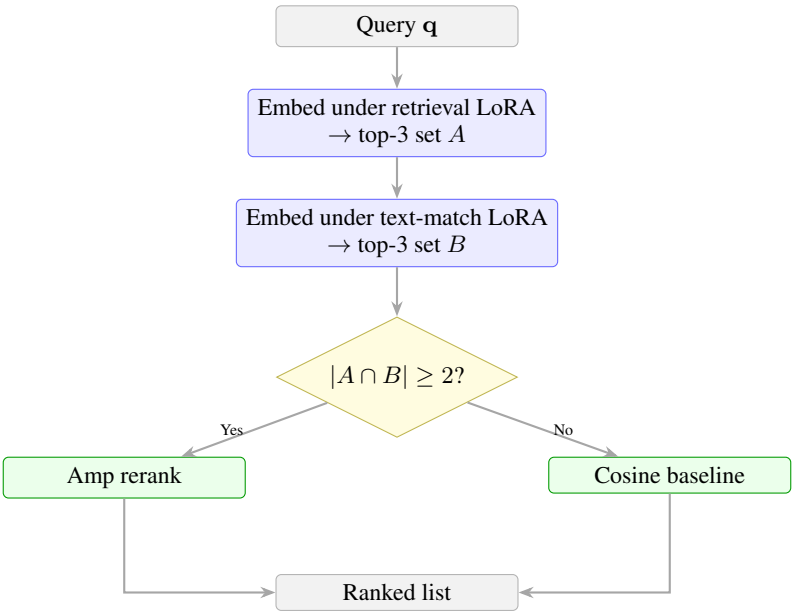

Figure 17: Program P47 (cross-LoRA top-3 overlap gate). Fires the amp only when the retrieval-LoRA and the text-matching-LoRA agree on the top-3 set. Established the cross-LoRA agreement pattern. Subsequent programs P49 and P110 extended this gate to triple-LoRA composition.

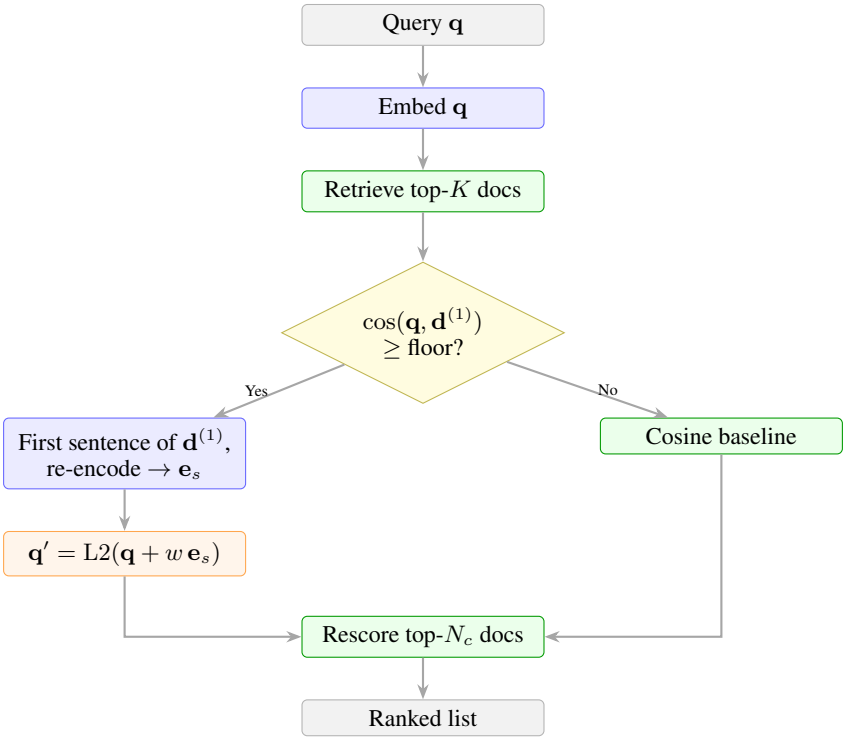

Figure 18: Program P76 (universal-min champion at $2\times$). Combines first-sentence anchor with a similarity-floor gate. The longest-defended $2\times$-cost universal-positive in the registry, with $+0.29$ nDCG@10 $\times 100$ minimum across all six universal cells.

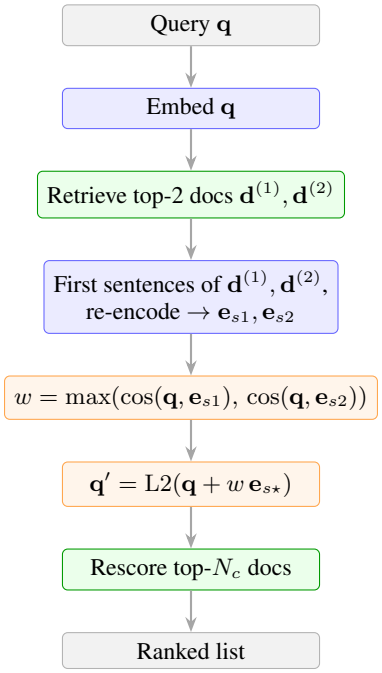

Figure 19: Program P97 (top-2 chunked anchor). Uses both the top-1 and top-2 documents' first sentences as anchors, max-pooling their similarities to the query before reranking. Captures the highest nano-SciFact delta of $+0.51$ nDCG@10 $\times 100$ among $2\times$-cost programs but breaks ArguAna because the top-2 is often a counter-argument with high cosine.

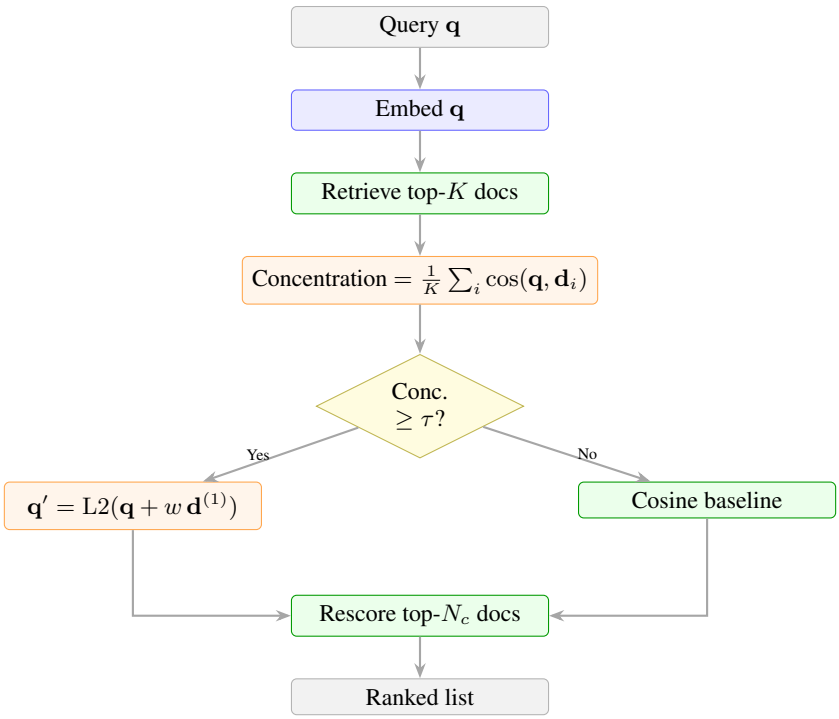

Figure 20: Program P102 (gap-concentration amp). Replaces the gap-confidence gate with a top-K concentration measure. The amp fires when the top-K similarity mass is concentrated above a threshold. A robustness-witness variant that maintains the AMP body but tightens the admit set.

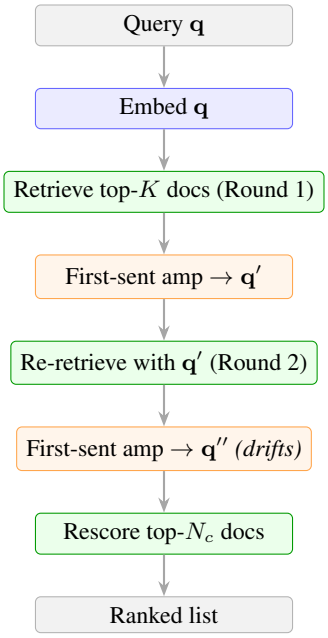

Figure 21: Program P103 (two-round first-sent amp). A multi-round member of the AMP family that re-retrieves with $\mathbf{q}'$ before the second amp pass. Like P40, the second round drifts the query off-manifold. The search moved beyond this direction.

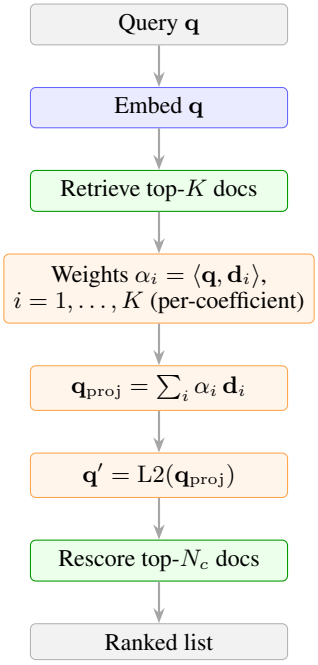

Figure 22: Program P164 (query-projection rotation). Projects the query onto the top-K subspace via the per-coefficient mean of $\langle \mathbf{q}, \mathbf{d}_i \rangle$ weights. A linear-algebraic alternative to the centroid update. Non-universal because over-rotation destabilizes SciFact ordering.

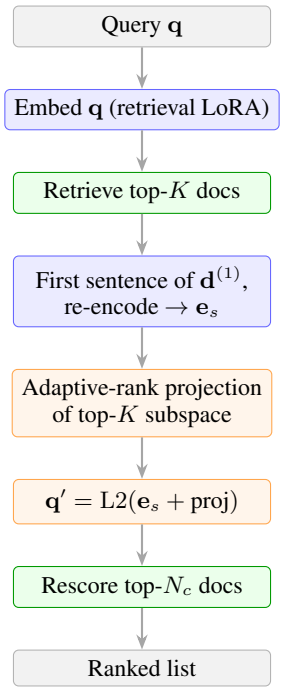

Figure 23: Program P171 (universal-avg champion at $4\times$). A composite anchor program combining the first-sentence body of P19 with adaptive-rank query projection. The longest-defended $4\times$-cost universal champion, with $+2.67$ nDCG@10 $\times 100$ average across all six universal cells.

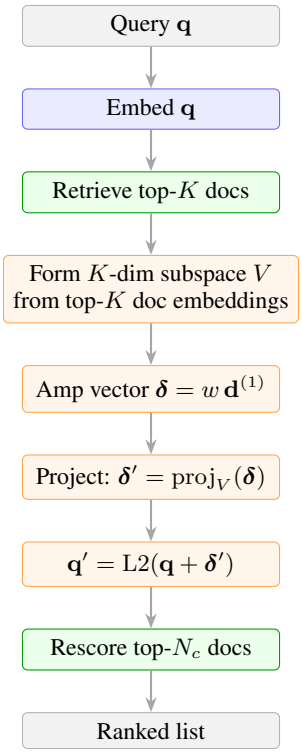

Figure 24: Program P174 (subspace-bounded amp). Restricts the amp update to lie within a K-dimensional subspace spanned by the top-K documents. Predecessor to the adaptive-rank P182 that became near-champion at $2\times$ before its small-SciFact regression was diagnosed.

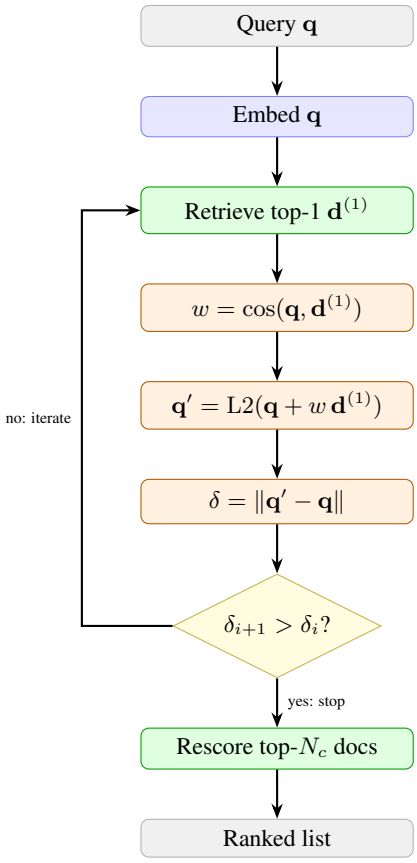

Figure 25: Program P28 (norm-convergence amp). Iterates the top-1 amp and tracks the update norm $\|\mathbf{q}_{i+1} - \mathbf{q}_i\|$. Stops the moment the norm increases (convergence reversal), with a safety cap of six rounds. Oracle-best on `j-v5-nano` ArguAna at $+7.18$ nDCG@10 $\times 100$. Cost $\leq 2\times$.

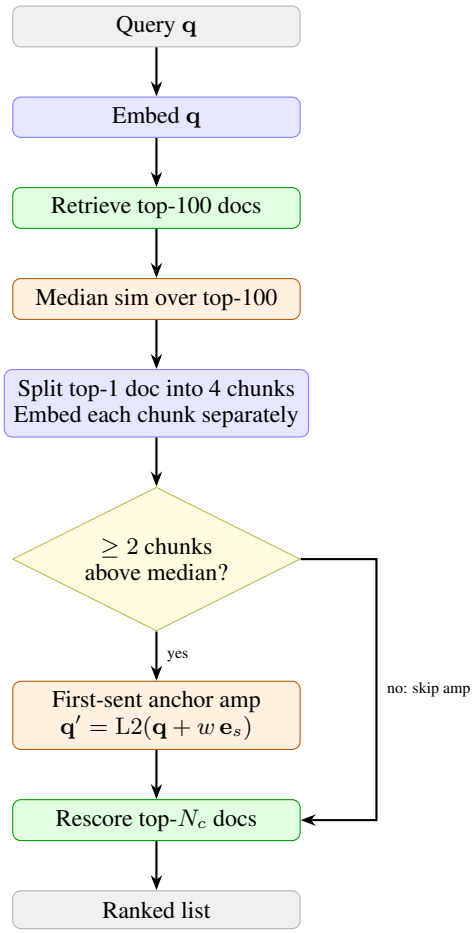

Figure 26: Program P77 (doc-chunk $K{=}2$ redundancy gate). Splits the top-1 document into four disjoint sentence-window chunks and encodes each separately. The amp fires only if at least two chunks have $\cos(\mathbf{q}, \mathrm{chunk}_i)$ above the per-query median similarity over the top-100 pool. Representative of the DOCCHUNK substrate family. Cost $\geq 4\times$.

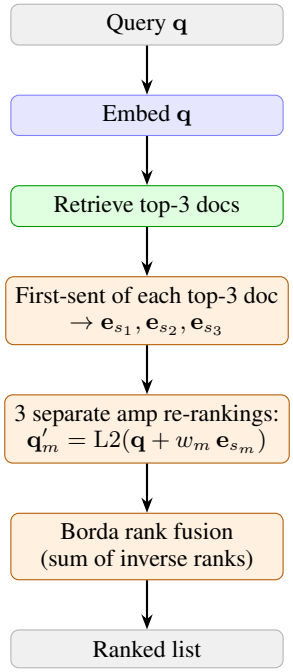

Figure 27: Program P37 (top-3 anchor Borda rank vote). Builds three separate re-rankings, each from amplifying $\mathbf{q}$ toward the first-sentence anchor of a different top-3 document. Combines the three re-rankings plus the baseline ranking by Borda rank vote. Representative of the score-space super-family. Cost $4\times$.

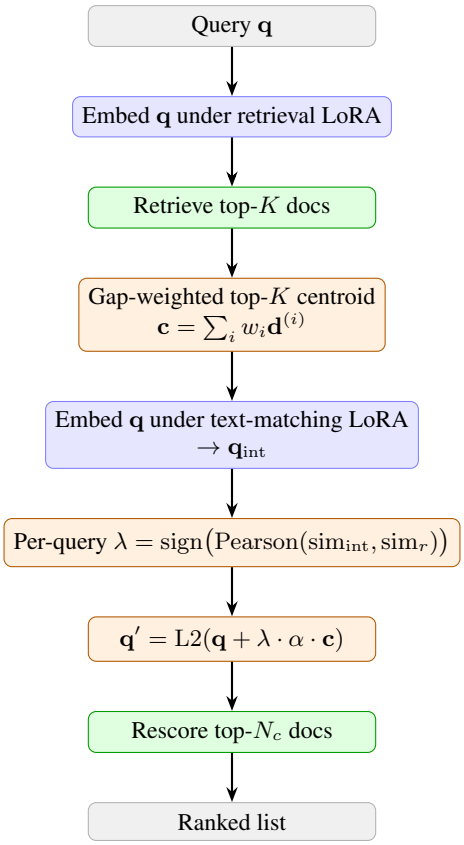

Figure 28: Program P203 (per-query lambda). Uses two LoRA adapters: the retrieval LoRA for the initial retrieval and centroid, and the text-matching LoRA for a per-query interaction signal. The sign of the Pearson correlation between the two LoRA similarity vectors determines whether the centroid update adds or subtracts. Oracle-best on `j-v5-nano` NFCorpus at $+1.69$ nDCG@10 $\times 100$. Cost $2\times$.

	NFCorpus		ArguAna	
	nano	small	nano	small
Vary α (K=3, τ=0.05):				
α=0.2	+0.87	+1.34	+2.25	+2.06
α=0.3	+1.32	+1.88	+3.21	+2.76
α=0.4	+1.61	+1.87	+3.64	+3.12
α=0.5	+1.52	+1.94	+4.01	+3.60
Vary τ (K=3, α=0.5):				
τ=0.05	+1.52	+1.94	+4.01	+3.60
τ=0.1	+1.46	+1.76	+3.28	+2.78
τ=0.2	+1.23	+1.30	+2.09	+1.95
τ=0.5	+1.11	+1.15	+1.48	+1.24
τ=1.0	+1.09	+1.17	+1.16	+1.02
Vary K (α=0.5, τ=0.05):				
K=3	+1.52	+1.94	+4.01	+3.60
K=5	+1.25	+1.67	+4.02	+3.52
K=8	+1.14	+1.40	+4.00	+3.53

Table 15: SOFTCENTROID component ablation, reporting Δ nDCG@10 ($\times$100) over the cosine baseline at each one-parameter sweep around the default K=3, α=0.5, τ=0.05. Interpolation α and temperature τ carry most of the gain. Centroid size K is largely inert.

Method	NFC	ArguAna	SciFact	FiQA	Mean
SOFTCENTROID	+1.49	+5.92	+0.17	+0.03	+1.90
(a) Alternative weighting schemes					
Uniform (=Rocchio)	+1.01	+2.33	+0.13	−0.37	+0.77
Linear	+1.05	+2.55	+0.12	−0.28	+0.86
Cosine[4]	+1.42	+3.34	+0.23	−0.27	+1.18
Hard top-1	+1.22	+7.48	−0.46	−0.45	+1.95
(b) Rocchio with negative centroids					
γ=0.2, N_{neg}=50	+1.25	+1.92	+0.12	−0.14	+0.79
(c) Iterative refinement (fresh re-retrieval)					
2 rounds (2× cost)	+1.40	+8.18	+0.04	−0.45	+2.29
3 rounds (3× cost)	+1.32	+7.83	−0.12	−0.47	+2.14
(d) Dimension masking (ECLIPSE/DIME-style)					
Variance mask (10%)	−0.13	−0.11	−0.23	−0.48	−0.24
Contrastive sub.	−3.64	−8.27	−3.95	−4.52	−5.09

Table 16: Extended baseline comparisons. Each entry is Δ nDCG@10 ($\times$100) over the cosine baseline, averaged across `e5-base-v2`, `j-v5-small`, and `bge-large-en-v1.5` on four BEIR tasks. SOFTCENTROID uses the default K=3, α=0.5, τ=0.05. The only alternative that exceeds SOFTCENTROID on mean Δ is hard top-1 replacement, which trades a +1.56 advantage on ArguAna for regressions on SciFact and FiQA. Iterative refinement at 2× cost gains on ArguAna but regresses elsewhere. Dimension masking consistently damages retrieval.

nanoBEIR Task	SC	SC_{K10}	$\text{SC}_{K5,\alpha.35}$
NFCorpus	**+0.58**	−0.47	−0.50
SciFact	**+0.55**	**+1.11**	**+0.26**
ArguAna	**+0.42**	**+1.78**	**+0.98**
FiQA-2018	**+1.66**	**+1.04**	**+2.47**
SCIDOCS	**+0.55**	**+0.85**	**+0.23**
MSMARCO	**+0.51**	**+3.86**	**+1.62**
Touche2020	**+0.25**	**+1.78**	**+0.37**
FEVER	−1.06	−1.06	−1.07
ClimateFEVER	**+1.07**	**+1.88**	**+1.89**
NQ	−0.42	**+0.86**	**+0.82**
HotpotQA	−1.31	−2.40	−3.10
Quora	−0.27	+0.01	+0.05
DBPedia	−0.55	**+0.70**	−0.03
Mean	+0.15	**+0.77**	+0.31
Median	+0.42	**+0.86**	+0.26
Pos cells	8/13	**10/13**	9/13

Table 17: Cross-model default-config validation on `e5-base-v2` across all 13 nanoBEIR retrieval tasks at the 50-query BEIR sub-sample, reporting Δ nDCG@10 ($\times$100). Three SoftCentroid variants from the `j-v5` frontier are applied unmodified. The K=10 variant is the strongest default on `e5-base-v2`, with a mean lift of +0.77 and 10 of 13 cells positive, reflecting that this embedding-model family produces a more diffuse local-cluster geometry than the `j-v5` retrieval LoRAs. Bold marks positive cells.

Encoder / variant	NFC	Sci	Arg	FiQA
`e5-base-v2` SC	$+\mathbf{0.58}$	$+\mathbf{0.55}$	$+\mathbf{0.42}$	$+\mathbf{1.66}$
`e5-base-v2` SC_{K10}	-0.47	$+\mathbf{1.11}$	$+\mathbf{1.78}$	$+\mathbf{1.04}$
`e5-base-v2` $\mathrm{SC}_{K5,\alpha.35}$	-0.50	$+0.26$	$+\mathbf{0.98}$	$+\mathbf{2.47}$
`bge-base-en-v1.5` SC	-0.14	-0.41	-1.28	$+\mathbf{0.93}$
`bge-base-en-v1.5` SC_{K10}	$+\mathbf{1.04}$	-2.81	-0.50	$+\mathbf{0.59}$
`bge-base-en-v1.5` $\mathrm{SC}_{K5,\alpha.35}$	$+\mathbf{0.24}$	-1.20	-1.42	$+\mathbf{0.46}$
`bge-small-en-v1.5` SC	-1.34	$+\mathbf{0.09}$	-0.76	$+\mathbf{0.97}$
`bge-small-en-v1.5` SC_{K10}	-0.75	-0.25	$+\mathbf{0.93}$	-0.09
`bge-small-en-v1.5` $\mathrm{SC}_{K5,\alpha.35}$	-0.45	-0.30	-0.62	$+\mathbf{0.63}$

Table 18: Cross-model transfer on the 4-task nanoBEIR probe at the 50-query slice. The table reports Δ nDCG@10 ($\times 100$) of SoftCentroid default and two FiQA-tuned variants on three monolithic embedding models. The full-BEIR validation in Table 5 uses `e5-base-v2` as the strongest of these three. Bold marks positive cells.